CHALMERS

Synthesis of mesoporous silica particles with control of both pore diameter and particle size

Master of Science Thesis in Materials and Nanotechnology program

ALBERT BARRABINO

Department of Chemical and Biological Technology
Division of Applied Surface Chemistry
CHALMERS UNIVERSITY OF TECHNOLOGY
Göteborg, Sweden, 2011

THESIS FOR THE DEGREE OF MASTER OF SCIENCE

Synthesis of mesoporous silica particles with control of both pore diameter and particle size

Albert Barrabino

Supervisor: Hanna Gustafsson
Examiner: Krister Holmberg

Department of Chemical and Biological Engineering

CHALMERS UNIVERSITY OF TECHNOLOGY

Göteborg, Sweden 2011

Synthesis of mesoporous silica particles with control of both pore diameter and particle size

Albert Barrabino

Department of Chemical and Biological Engineering
Division of Applied Chemistry
Chalmers University of Technology
SE-412 96 Göteborg
Sweden
Tel. +46 (0) 31 772 10 00

Cover: TEM and SEM images different samples of mesoporous silica particles.

Göteborg, Sweden 2011

Synthesis of mesoporous silica particles with control of both particle diameter and particle size

Albert Barrabino
Department of Chemical and Biological Engineering
Division of Applied Chemistry
Chalmers University of Technology

Abstract

During last years the interest for nanotechnology and mesoporous silica materials has increased due to benefits that these materials can provide. Typical characteristics of mesoporous materials are a large surface area and pore volume, well-ordered and uniform pores with adjustable pores between 2 and 50 nm. Pore dimensions are comparable to many biological molecules, like enzymes, and may therefore be suitable as a support in enzyme encapsulation

The aim of this project was to synthesize mesoporous particles with a fixed pore size in order to optimize enzyme encapsulation. The specific pore size was determined based on previous studies on encapsulated lipase from *mucor miehei* where the optimal pore size was found to be ~9 nm. Through this project different synthesis has been studied, different types of surfactants have been used (Pluronic 123, CTAB) as well as different types of silica sources such as TEOS or sodium silicate solutions. The synthesis conditions have been varied in order to study the effect on the particle and pore size.

In this work really small particle sizes were synthesized. Spherical 40 nm nanoparticles was obtained using octane as a hydrophobic support and styrene as a mesoporous template. However, the pore structure was rather slit-shaped than cylindrical. A perfect pore structure and size was reached using a sodium silicate solution as silica source, pluronic 123 as a pore template and an aging period of 24 hours at 180°C. The particles obtained in this synthesis varied with a diameter up to values around 200 nm.

TABLE OF CONTENTS

1. INTRODUCTION

We could define nanotechnology as "the creation of functional materials, devices and systems through control of matter on the nanometer length scale (1 – 100 nanometers), and explotation of novel phenomena and properties (physical, chemical, biological, mechanical and electrical) at that length scale" [1]. We also could say nanotechnology is the reason of the development of "applied surface science" [2].
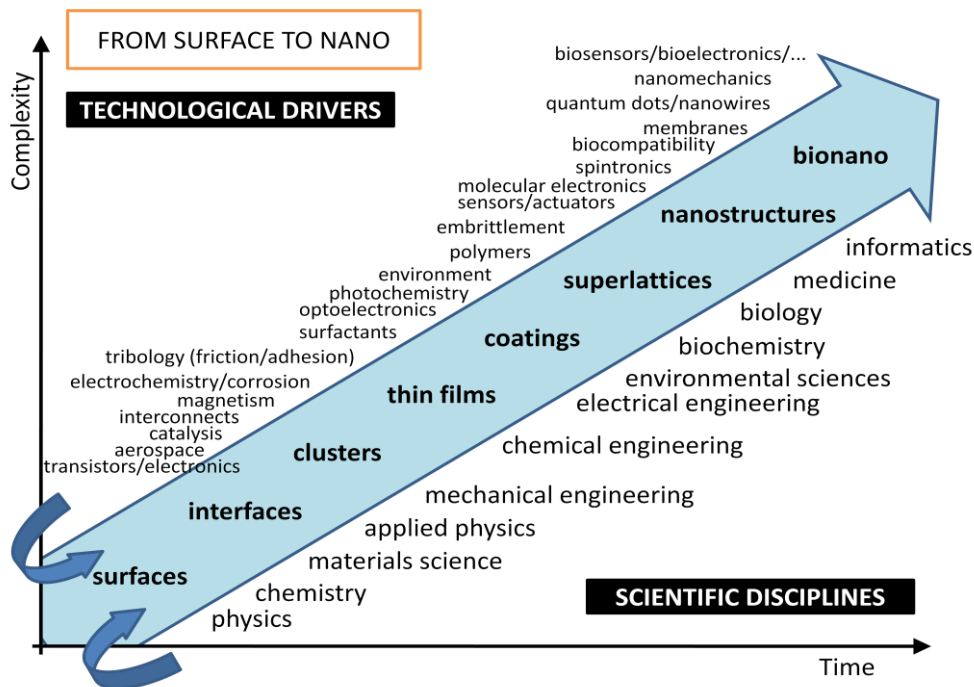
Figure 1. Historical evolution of surface science toward nanochemistry. The time period corresponds to about 50 years, beginning about 1950 [2].

There is much debate on the future implications of nanotechnology. With the prefix "nano" is being carried out a scientific-technological revolution. Nanomachines, nanoelectronics, nanodevices, nanostructured materials, they will definitely help on the progress and evolution of our society. Although nanotechnology is a really "young" area and it is expanding quite fast due to their unlimited applications and the several number of improvements that they are bringing to us. One of these interesting and booming applications is the materials science, which is based this thesis.

1.1. Background

Interest in nanotechnology and mesostructured silica materials has soared in the recent years. This new generation of materials offers us endless possibilities in a variety of sectors and applications. Maybe, the concept of nanotechnology was born with the zeolites. In 1925 it was discovered that zeolites have selective adsorption properties, and in 1932 we can hear about the concept of *molecular sieve* for the first time. However, zeolites have small pores and diffusion of particles with a diameter larger than 1.2 nm will not be possible. In this moment is when the concept of mesoporous became important.

The word *meso* is referred to one specific range of pore size from 2 to 50 nm. These mesostructured materials are made of amorphous silica, and they were discovered in the beginning of the 90's. Since that time, the interest in these new materials has been increased in a considerably way.

The unique properties of mesoporous silica materials are used to immobilize enzymes. Enzymes are really interesting nowadays due to their increasing applications in chemical and pharmaceutical industries to prepare a wide variety of products, such as biosensors or drugs [3]. For example lipase is really interesting for industries such as food, pharmaceutical, detergent, textile and paper [4, 5]. However, enzymes are difficult to recover and recycle if they are free in solution. In this point is when mesoporous materials take part of the game. They can increase the enzyme stability and they make the recycling process much easier if the proteins are encapsulated inside them. Their pore size range makes mesoporous materials perfect for this purpose, encapsulation of enzymes. Especially the case of SBA-15 materials, conformed by using a triblock copolymer such Pluronic P123 which have a pore size range between 5 to 30 nm [5]. This range makes SBA-15 materials perfect for the encapsulation of enzymes.

1.2. Aim

This Master Work Thesis has as an objective to control the formation and growth of mesostructured silica particles, moreover in the reduction of the particle size keeping a proper good mesoorder, for further applications. The purpose for these particles was the encapsulation of enzymes into their pores, in particular for lipase. Being the application of silica the most important point to consider, was to try different methods of synthesis, always chasing to reach the lowest particle size as possible with a well-ordered pore structure. In this manner the most important point of this work was not to find the formation mechanism of the mesostructured materials. This aim drove the work through different procedures, different reactants, different conditions of synthesis, etc. All these studies are presented in different sections depending on the different synthesis and procedures.

2. SILICA MESOPOROUS MATERIALS

2.1. Introduction

Mesoporous materials consist of inorganic metal oxides, like silica or alumina, and have pore sizes in the range of between 2 and 50 nm. They are synthesized by using a surfactant forming regularly aligned assemblies that are used as a template for the metal oxide, followed by template removal. They are also water soluble, chemically and thermally stable with mechanical strength and are toxicologically safe. At the surface of the mesoporous silica materials there are silanol groups that can be utilized for enzyme immobilization by hydrogen bonding between hydroxyl groups and carbonyl or amino groups on enzyme molecules.

The surfactant is crucial in the synthesis since it will decide the size of the formed pores and a wide variety of different surfactants can be used.

The main surfactant used in mesoporous synthesis is non-ionic block copolymers. Advantages with block copolymers are their stability to time the ordering by varying solvent composition, molecular weight or copolymer composition. The size of the pores can also be regulated by using different temperatures during synthesis, where high temperature gives larger pores.
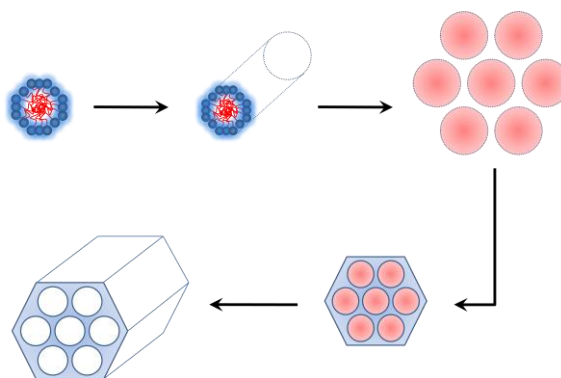
Figure 2. Schematic representation of the formation of MCM-41 materials. [7]

This mechanism was proposed by *E. Davis et al.* in 1993 [6], where silica is arranged in liquid crystal template, made by CTAB.

It could be interesting to do a fast and simple classification of mesoporous materials according to this work. Silica Mesoporous Materials are synthesized using amphiphilic molecules as a template for their internal structure. At the beginning cationic

surfactants were used to create these materials. Varying the conditions of the syntheses we could obtain two different types of internal structures: two-dimensional hexagonal structure (*p6mm*) also known as MCM-41 [7, 8]; tridimensional cubic structure (*Ia$\overline{3}$d*), known as MCM-48. When we got a two-dimensional hexagonal structure, but instead of a cationic surfactant we use a tribloc copolymers such Pluronic P123, that material is also called as SBA-15 [9, 10].

SBA materials have been reported as hydrothermally more stable due to their thicker walls [11]. The structure of the surfactants used in these materials is *(EO)$_x$-(PO)$_y$-(EO)$_x$*. When *x* has a value between 17 and 37, then we get SBA-15 materials. X also affects on the wall thickness. The value of *y* has more relation with the pore size of the material. Another advantage of SBA-15 materials is that they have disordered micropores, which allows the connection between mesopores [11].

2.2. Surfactants

Surface active agents, or also known as surfactants are molecules that have tendency to adsorb at the surfaces and interfaces. They have a dual chemical structure, one part of the molecule is hydrophilic and the other is hydrophobic. Surfactant with amphiphilic character adsorb on the interface to reduce the free energy of phase boundary. In the next figure is possible to watch the structure of one surfactant:
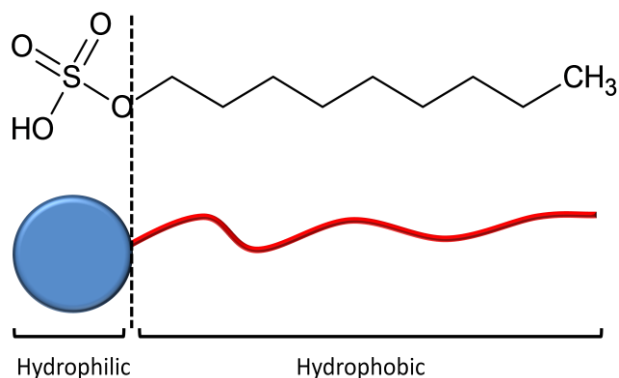
Figure 3. Basic schematic of a surfactant.

Basically, the surfactants could be in three forms: some solubilised in water as single molecules; others are in the interface water-air and they could be in the interface water-solid recipient. After reached the saturation of all those interfaces, the entire surfactant remaining in the water is on form of clusters called micelles. This point, when the first micelle is formed, is called Critical Micelle Concentration (also known as CMC). The CMC depends on chemical structure of each compound, for instance, on the length of the hydrophobic tail, as much longer, lower the CMC. This phenomenon can be explained because the longer carbon chains are trying to get together, this implies a lower energy and therefore more stable systems. CMC is a really important value for surfactants. [12]

One popular way to classify the surfactants is according to their charge in the polar head. Then, we can make these 4 groups:

- **Anionics:** this family of surfactants has negatively charged polar head groups. The non-polar group is used to be a large hydrocarbon chain between C12 and C18 range. The polar groups mostly used in this kind of surfactants are carboxylates, sulphates, sulfonates and phosphates.

- **Cationics:** they have a positive charged polar head group and a large alkyl chain as a non-polar group. This family are based on nitrogen atom. Amine and quaternary ammonium-based products are common as a head group.

- **Non-ionics:** non-ionic surfactants have a polyether or a polyhydroxyl unit as the polar group. Actually the poly(ethylene oxide) is the most common polar group. As a non-polar group poly(propylene oxide) is probably the most common. In this family, we should emphasize on the block copolymers. These copolymers have a relatively low molar mass. They are composed by blocks of different polymerized monomers.

- **Zwitterionics:** This is the last family of surfactants. They have two different charges of different sign on their head group giving a neutral charge. The most common positive charge is given by an ammonium group, the source of negative charge may vary, but carboxylate is by far the most common.

In this work, we have been working basically with these surfactants: CTAB (*Cetyl trimethylammonium bromide*), which is a cationic surfactant; the block copolymer Pluronic® P123, which is a nonionic surfactant.
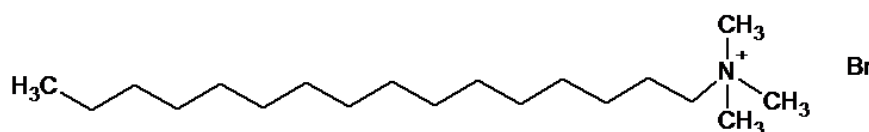
Figure 4. Chemical structure of CTAB.

CTAB is a quaternary ammonium compound, which are not sensitive to pH as well as are the amines. The counterion used in this compound is bromide. This family of surfactants have been widely studied in the formation of mesoporous silica-based materials [14].
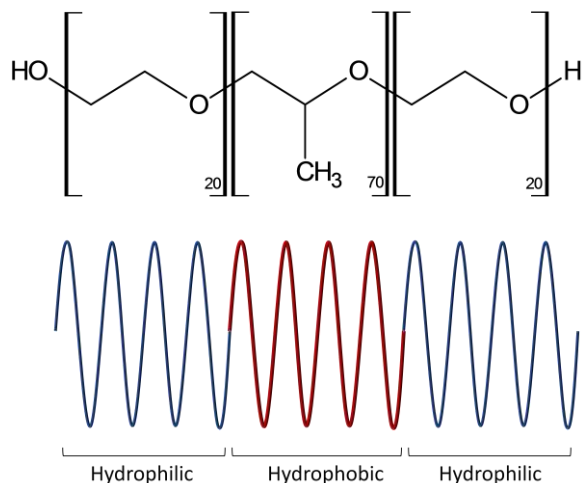
Figure 5. Chemical structure of Pluronic 123.

The poly(ethylene oxide) PEO is the hydrophilic part of the molecule and poly(propylene oxide) PPO is the hydrophobic. These different parts give the polymer an amphiphilic character. These kinds of copolymers are named by BASF as Pluronic®. Different types of PEO-PPO-PEO have been studied in different papers [10, 13]. After reached the CMC, if we increase the surfactant concentration, depending on the type of surfactant and temperature, we may lead the growing of the micelles. Then, interaction between these micelles can provide us different types of structures in the solution. These structures are called surfactant liquid crystals. The different liquid crystal structures that a surfactant can give are gathered in phase diagrams. In the next figure we can see the phase diagram for the Pluronic P123.
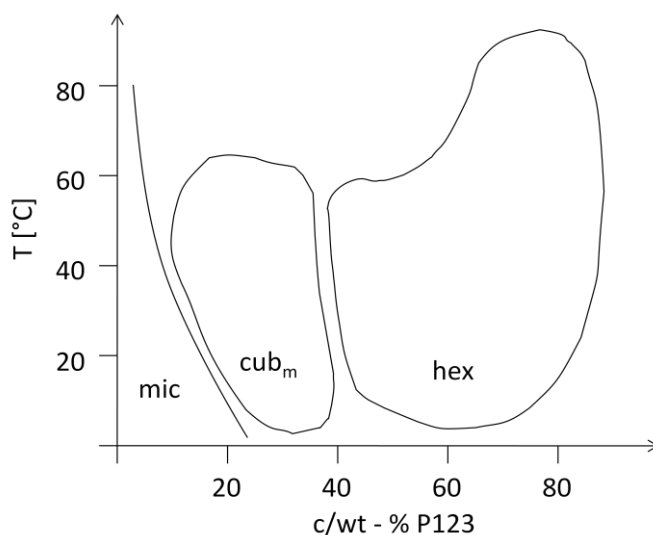
Figure 6. Phase diagram for Pluronic P123 [13].

Due to this behaviour, surfactants are used as a mesoporous template in the synthesis for the mesoporous materials [14, 15]. For instance, according to the diagram above we can synthesize different silica mesoporous materials using Pluronic® P123 with different internal structures, cubic and hexagonal.

2.3. Routes

In this work we have worked basically with four different syntheses. We could differentiate these syntheses depending on the silica source, for instance. Essentially all the synthesis has the same principle, the addition of one silica source into a surfactant template in water solution. In the scheme below can be appreciate the procedure to synthesize mesoporous materials.
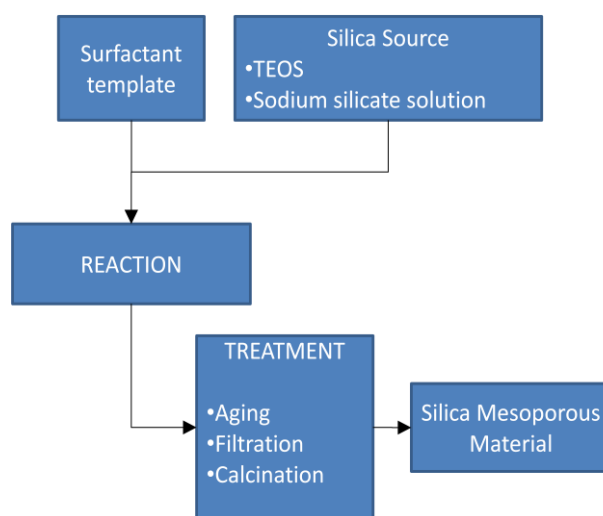
Figure 7. Basic reaction scheme.

All the routes have the same essence. In one hand we should create a template for the mesostrucure, we can do that dissolving a surfactant (Pluronic® P123 and CTAB in our case). In the other hand we have to prepare a silica solution, it could be from an inorganic source, as sodium silicate solution, or from an organic source as TEOS. In both cases we should reach a low pH value. Hydrolysis in acidic media allows the protonation of the TEOS. When it is protonated, the silicon atom becomes more electrophilic and it is easier to be attacked by water. In acidic media the velocity of hydrolysis is much higher compared to more basic pH [9, 16-18]. Low pH values also help to reach more ordered materials [9-11]. Since all the conditions for the synthesis are reached, we are mixing both solutions under vigorous stirring during *X* hours. After that the mixture has to be aged in autoclaves. This process allows to control the pore diameter. The last step for the basic synthesis is the collection of the particles and the calcinations in order to remove of the surfactant template to get finally the mesoporous material.

2.4. Silica-protein interactions

The interactions between silica and other particles such enzymes can be ionic, polar and lipophilic. At the surface of silica, silanol groups can be found. These groups can be used to fix enzymes by hydrogen bonding between hydroxyl groups and carbonyl or amino groups in the enzyme molecules [19].

2.5. Applications

Silica Mesoporous Materials can provide our society with several advantages. Mesoporous silicates synthesized by using a surfactant template method are really stable, and they have narrow pore sizes. They can be used in different fields, such separation techniques, adsorption, catalysis, drug delivery, sensors, or photonics for instance.

In the field of biocatalysis or drug delivery, these materials are interesting due to they could be used to encapsulate proteins inside their pore structure. If these proteins were encapsulated into mesoporous materials, their stability would be increased (due to the protection that the mesoporous materials provide) as well as recycling possibilities.

The characteristics for these mesoporous silicates have to be optimum in order to protect the enzymes but at the same time allow some movement of the enzymes and diffusion of substrate into the pores. That requires an optimum pore size. If the pore diameter is large, the diffusion rate of the substrate into the pores is high and we can reach a higher product formation, on the other hand large pore sizes contributes to increase the leaching of the enzymes since they are weakly adsorbed to the surface. If the pore diameter is narrower, the lipases would be more protected, the leaching would be reduced as well as we will get an enhanced hydrothermal stability [21], but at the same time they will block the pass of the reactants trough the pores. [5, 22]

We should talk about the particle size and its importance. During encapsulation enzymes only reach short distance down the pore, it means that with smaller particles we would get a higher loading capacity. In addition reducing the particles size we are increasing the contact area [5].

3. ANALYTICAL TECHNIQUES

In this section we will introduce the different analytical techniques used in this work for characterizing the samples. These techniques range from N_2 adsorption to electron microscopy (TEM and SEM).

3.1. Electron Microscopy

The first electron microscope was designed and built between 1925 and 1930 by Max Knoll and Ernst Ruska. An optic microscope is limited for the wavelength of the visible light. Electron microscopy uses an electron beam to see the objective instead of photons or visible light but it operates in the same principles. There are different types of electron microscopy but all of them are associated to the electron wavelength. The resolution of those devices is the order of few Angstrom (10^{-10} m), which is interesting for the study the details of a cell or different materials down to near atomic levels.

Electron Beam

Thin sample
10-200 nm

Elastically scattered electrons

Inelastically scattered electrons

Unscattered electrons

TEM, HREM, ED

EELS, EFTEM
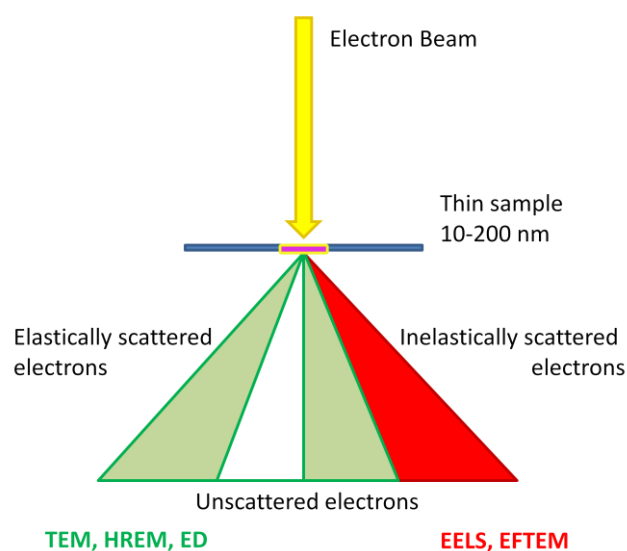
Figure 8. Electron interactions with surfaces [23].

The electron beam is generated by an electron gun, accelerated using a high voltage. Electromagnetic lenses are used to focus the electron beam into a thin beam. These devices are always working under High vacuum conditions (typically working on the

order of 10^{-4} Pa) due to the air affects on the electron behaviour and we only need an interaction between the beam and the sample [23].

3.1.1. Transmission Electron Microscopy (TEM)

This kind of microscope allows us to see the internal structure of our materials. The way it runs is the described above. After the beam interacts with the sample, depending on the density of the material, some electrons are scattered and they go out of the beam disappearing. The unscattered electrons impact against a fluorescent screen which gives the image of the specimen [23]. This technique is widely used to investigate nanostructures [24].
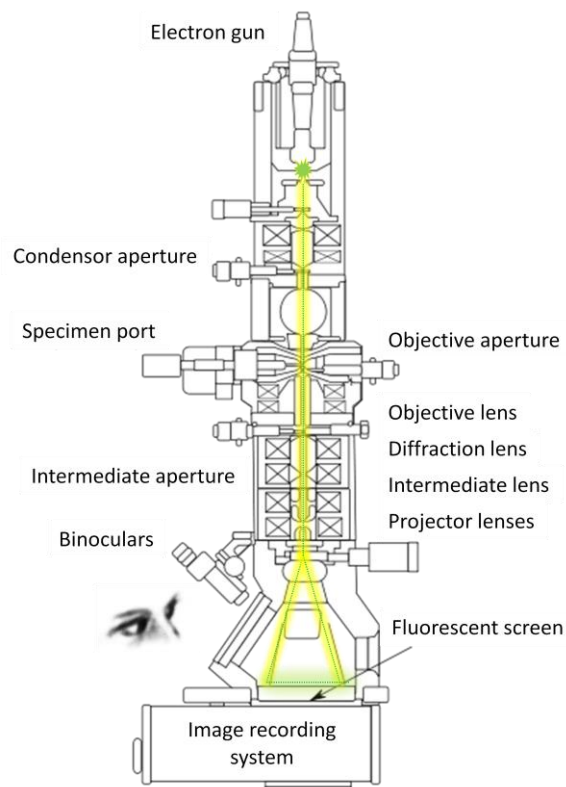
Figure 9. TEM parts.

3.1.2. Scanning Electron Microscopy (SEM)

The scanning electron microscopy is a type of electron microscope. It uses high-beam energy of electrons such as TEM. The difference between them is that SEM has special detectors for elastic scattered electrons, inelastic scattered electrons and for the emission of electromagnetic radiation instead of the unscattered electrons, such TEM does. In this manner SEM can provide the topography of the sample's surface, composition and electrical conductivity for instance.

To be able to generate a view of the sample using SEM, this has to be electrically conductive, or at least at the surface of the sample. If they are not, the samples should be coated with a metal such gold, the most common used.

This device can show details smaller than the range between 1 and 20 nm, depending on each instrument.

3.2. Dynamic Light Scattering (DLS)

This is a technique in physics, used to determinate the size of the particles and aggregates giving us the size distribution profile.

When the particles are smaller than the light wavelength (below 250 nm) these are able to scatter the light in all directions. If the light source is a monochromatic (same frequency) an coherent laser (same wavelength) , the observed scattering intensity becomes time-dependent. This effect is due to the small particles are undergoing *Brownian motion*. The *Brownian motion* defines the random movement of the particles suspended in a fluid. It means that the distance between the particles which scatters the light is constantly changing with time.

For the data analysis CONTIN METHOD was used [25]. This method is ideal for heterodisperse, polydisperse and multimodal systems.

3.3. Small angle x-ray scattering (SAXS)

SAXS or small angle x-ray scattering is one technique based on the elastically scattered x-rays. It is a fundamental method for structure analysis of condensed matter. The sample is illuminated by x-rays and the scattered radiation is registered by a detector. X-ray is a kind of electromagnetic radiation with a higher energy than ultraviolet radiation, this is absorbed by core electrons (electrons that do not participate in the bonding). This technique is recorded using a low range of angles, between 0.1° to 10°. SAXS give us information about the characteristics of the structure of our sample, such to determine the particle shape or the size distribution [26, 27].

3.4. N_2 Adsorption

This technique allows to calculating the specific surface of a sample based on the adsorption of nitrogen molecules at the surface. This theory is also known as BET, which is based on one monolayer adsorption on the surface, an extension of Langmuir theory [28].

We call isotherm to all the equations which relate the surface recovery with the pressure at constant temperature [29]. There are a lot of expressions for isotherms, but the most used is the Langmuir's Isotherm [30].

$$\theta = f(P) \ at \ constant \ T$$

$$\theta = \frac{kP}{1 + kP}$$

Langmuir's Isotherm is an expression for monolayer, but BET introduces the concept of a multilayer adsorption which the following hypothesis:

- The molecules are adsorbed infinitely in layers on the solid surface.
- There is no interaction between the different adsorbed layers.
- The Langmuir's theory can be applied on each layer.

The BET (Brunauer, Emmett and Teller) equation is:

$$\frac{\frac{P}{P_0}}{n_a\left(1-\left(\frac{P}{P_0}\right)\right)} = \frac{1}{n_m \cdot C} + \frac{C-1}{n_m \cdot C} \cdot \frac{P}{P_0}$$

With:

n_a = adsorbed amount.
n_m = monolayer capacity.
C = BET constant.

The IUPAC classify the physisorption isotherms in six types shown in the figure below. In our work we will get the type IV isotherm which presents a hysteresis loop. Type IV is the typical isotherm for mesoporous materials. Hysteresis loop is due to the capillary condensation taking place in the mesopores, and the first part of the curve is attributed to the monolayer adsorption [31]. Thus, hysteresis loop is a sign of porosity. They show a wide variety of forms.
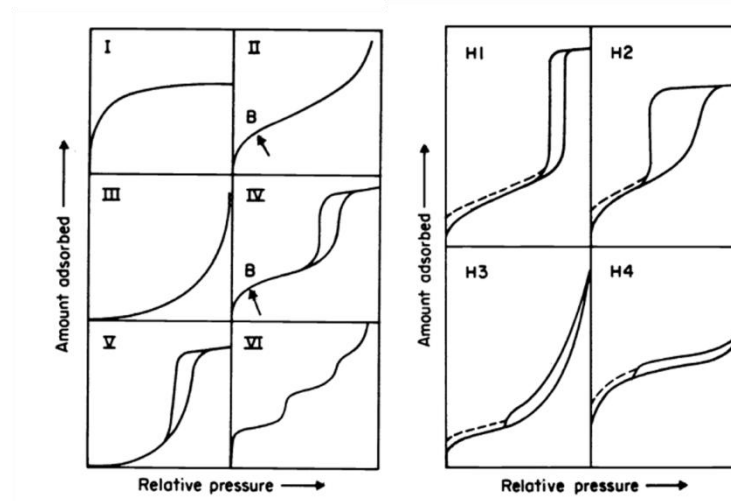
Figure 10. IUPAC Isotherms types and types of hysteresis loops [31].

Nevertheless, the factors on adsorption hysteresis in not completely understood.

3.5. Freeze Dryer

The freeze dryer uses a lyophilisation process to remove all the water inside the sample without damage the structure of our samples. This technique works freezing the sample and then makes water sublime from solid phase to gas phase reducing the pressure to low values, by application of vacuum. It's needed a fast freezing of the sample using liquid nitrogen in order to avoid the formation of ice crystals, which can damage the internal structure of the sample. The temperature reached is surrounding -90 degrees. This procedure can last for several days, is a slow process.
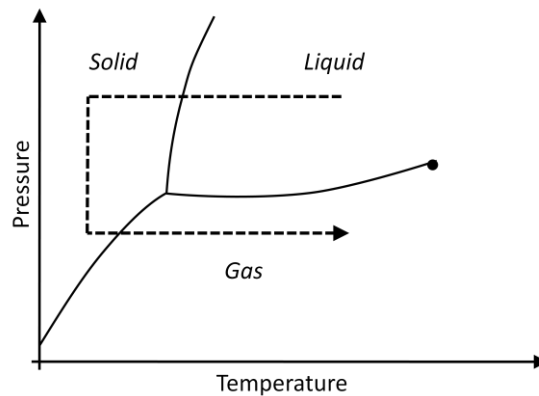
Figure 11. Route followed by water in a freeze dryer instrument.

3.6. Fourier Transform Infrared Spectroscopy (FTIR)

This technique tells us how one sample absorbs light at each wavelength, so it is an absorption technique. FTIR is also a chemically-specific analysis technique. It can be used to identify chemical compounds and substituent groups. An infrared light is used, this light occurs between 0.7 and 500 μm (between microwaves and visible spectrum). We could say that is a kind of vibrational spectroscopy. When the incoming infrared photon interacts with the molecule, this one can absorb the energy and vibrate faster and there is a transition in the molecule to the next vibrational energy state. So, the absorption leads to increase the vibrational energy level.
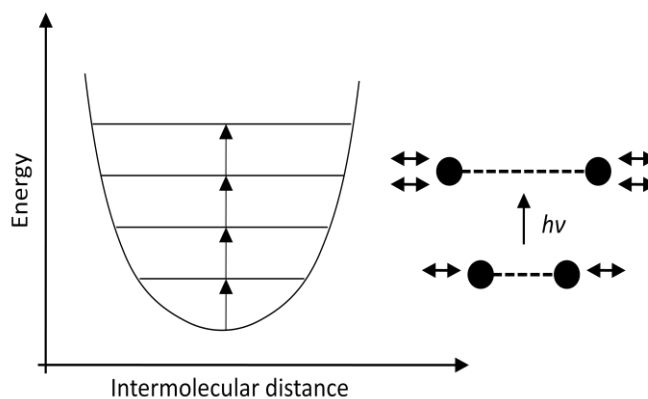
Figure 12. FTIR basic effect on the atoms.

After the detector collects the data coming from the sample, a mathematical algorithm is needed in order to proceed the data into the spectrum. This algorithm is the Fourier Transform. Every compound has their own spectrum, it is kind a fingerprint, this makes FTIR useful for several types of analysis.

4. EXPERIMENTAL

In this work different synthesis has been used to obtain mesoporous silica particles with varying properties. We will describe the setups for each one in this chapter. First we may say that we have been working with 4 different syntheses during the thesis. We will name them synthesis I, II, III and IV. Synthesis I and IV are quite similar to each other with smooth variations between both. In synthesis II another source of silica was used, a sodium silicate solution, and the procedure was completely different. For the synthesis number III we used again TEOS as a silica source but we used polystyrene as a template for the mesopores.

4.1. Chemicals

$EO_{20}PO_{70}EO_{20}$ (Pluronic® P123, M_n ~5.800 Sigma-Aldrich), TEOS (ReagentPlus®, ≥99,9%, Sigma-Aldrich), n-octane (anhydrous, ≥99%, Sigma-Aldrich), l-lysine (≥98%, Sigma-Aldrich), Styrene monomer (ReagentPlus® ≥99 %, Sigma-Aldrich), 2,2'-Azobis (2-methylpropianoamidine) dihydrochloride (97% granular, Sigma-Aldrich), CTAB *Cetyl trimethylammonium bromide* (≥98 %, Sigma-Aldrich), NH_4F (≥99,9%, trace metal bases, Sigma-Aldrich), Sodium silicate solution (10,6 % Na_2O – 26.5 % SiO_2, Reagent grade, Sigma-Aldrich), Potassium Chloride (Reagent, 99.0-100.5 %, Sigma-Aldrich).

4.2. Reactions setups

These synthesises were running under vigorous stirring at constant temperature during X hours. The reaction was simple, only a mixture of all reactants and chemicals in a constant temperature. So for both synthesises we used a round-bottom flask on a silicon oil bath in order to keep the temperature constant during the operation.

4.2.1. Synthesis I

In a typical synthesis, Pluronic P123 ($EO_{20}PO_{70}EO_{20}$) was used as the hexagonal template and a structure agent directing. In a typical synthesis 4 g. of Pluronic P123 was dissolved in 120 ml of HCl (2M) and 30 ml of deionized water, stirred vigorously and heated up to 35 °C. Then 8 g of KCl were added to the mixture. The reaction took place for 20 h. under continuous stirring. The mixture was aged on stainless steel pressure autoclaves with Teflon containers for 24 h. at 100 °C. The particles were collected by filtration and cleaned with deinozed water. Then they were calcined from room temperature to 550 °C for 8 h. followed by heating at 550 for 6 h. more.

4.2.2. Synthesis IV

As a typical synthesis 3 g of P123 were dissolved in 63 g of HCl (2M) and 35 g of water. The mixture was heated at 25 °C and stirred vigorously during the entire process. 0.031 g of NH_4F were added to the initial mixture. After 10 min a mixture of octane and TEOS was added (12 g of octane and 4 g of TEOS). The reaction took place for 24 hours at constant temperature and vigorous stirring followed for 24 hours in an autoclave at 140°C. The particles were collected by filtration and washed with water and then calcined from room temperature to 550 °C for 8 hours followed by heating at 550 °C for 6 hours more.

4.3. Synthesis II

Synthesis II was a bit different from the others. In this one we used an inorganic silica source such a sodium silicate solution. The first procedure was preparing the silica solution, thus require to reaching an acidic pH (between 2.8 or 3.0). For that purpose we used a strong ion-exchange resin (*Amberjet 1500*). The next step is a simple mixing of the silica solution with the surfactant template.

In a typical synthesis 22.64 ml of water glass were diluted to 100 ml with deionized water. The solution was washed for 8 – 10 minutes in a strong acid cation exchanger (*Amberjet 1500H*). A solution with pH 3 was obtained. As a typical synthesis 4,57 g of acidic silica solution were mixed with 5,80 g of P123 solution (5 wt.%) and 19,62 g of deionized water. After 3 days, the samples were freeze dried and then calcined in the oven from room temperature to 550 °C for 8 hours followed by 6 hours heated at 550°C.

4.4. Synthesis III

The third synthesis needs a little bit more complicated system. It needed a non-reactive atmosphere, which was achieved using N_2. This setup was composed by a three-necked reactor, a silicon oil batch with a heater and a reflux column.

We created a nitrogen flow through our system to create the inert atmosphere. This way we could avoid the oxidation of the styrene.

Water was used as a cooler for the system.
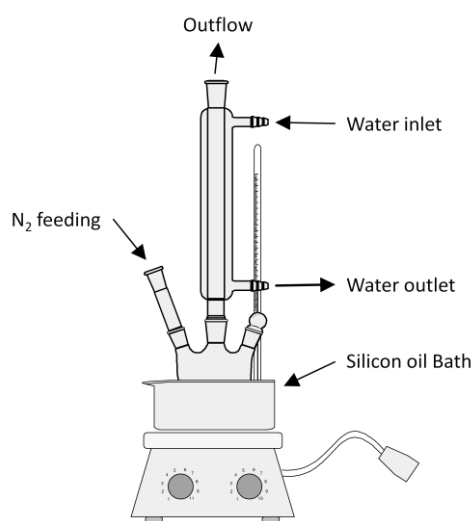
Figure 13. Synthesis III Scheme.

In a typical synthesis mesoporous particles were synthesized at 70°C under nitrogen atmosphere for 20 hours. As a typical synthesis 0.4 g of CTAB, 24 g of octane, 0.09 g of l-lysine and 124 g of water were mixed under vigorous stirring. The styrene monomer was pre-washed with one solution of 2.5 M NaOH in order to remove the stabilizer. After a clear solution was obtained 3.3 g of styrene monomer, 4.0 g of TEOS and 0.14 g of AIBA were added to the mixture. After the reaction time, the heating was stopped and the suspension was cooled down naturally to room temperature and then the suspension was decanted for one overnight. The organic phase was separated and dried naturally inside one fume hood. Once dried the sample, it was calcined from room temperature to 550 °C for 8 hours followed by heating at 550 °C for 10 hours.

5. RESULTS AND DISCUSSION

5.1. Synthesis I

Since mesoporous materials such MCM-41 were discovered by *Mobil Research Corporation* in 1992 [7], a new world of possibilities was opened up in front of us. The same year *Zhao et al.* introduce the SBA-15 materials [9, 10]. As we said before, these new materials became really useful for several applications. Now, the aim of this work was reduce the particle size of those particles according to all the advantages we talked about before. We based the first synthesises on the typical one introduced by *Zhao et al.* on 1992 [9, 10]. The main problem was these particles have an average size of 1 μm and they show aggregation problems. In this section we tried to fix the aggregation problem and reduce the particle size as much as we can.

It has been reported before that adding salts to the reaction such NaCl, contribute in create and interaction on the silica gels [32], giving as a result aggregates between the particles after the whole process. The effect of the inorganic salts on the formation of silica has been studied widely before [32-34].
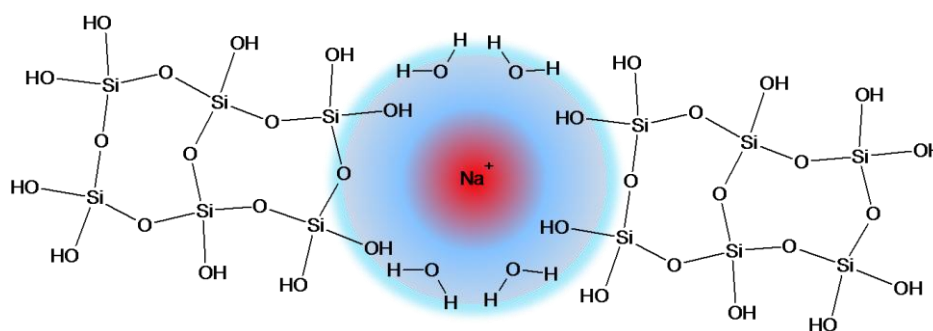
Figure 14. Effect of Sodium counterions between two silica particles [32].

Sodium ions are small, when Na^+ is absorbed on the silica surface these can coordinate with the oxygen atoms from the silanol groups between two particles and surface-bonded water. Thus a linkage between particles can be reached. But K^+ ions are different. Potassium ions are larger than sodium ions, and they are weakly hydrated. These ions also are absorbed on the particle surface creating a layer covering all the negative charges on the silica surface. Despite K^+ counterions cannot act as a bridge between two silica particles, due to their larger size and their weak hydration as we said
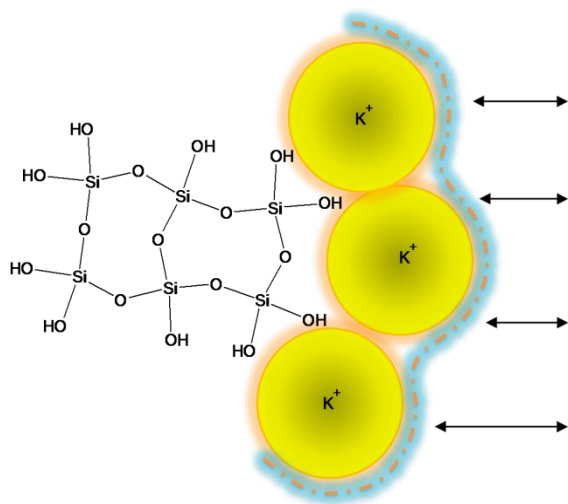
above, the layer absorbed on the negatively silica surface will create a shield on the particle surface. So a repulsive force between particles can be reached by using potassium counterions [32]. This shield helps to avoid the creation of aggregates between the silica particles.

The synthesis was varied, in order to study if it possible to reduce the particle size, by either changing the surfactant/silica ratio or diluting the mixture from 30 g water to 100 g water.

Figure 15. Effect of potassium counterions on a silica particle [32].
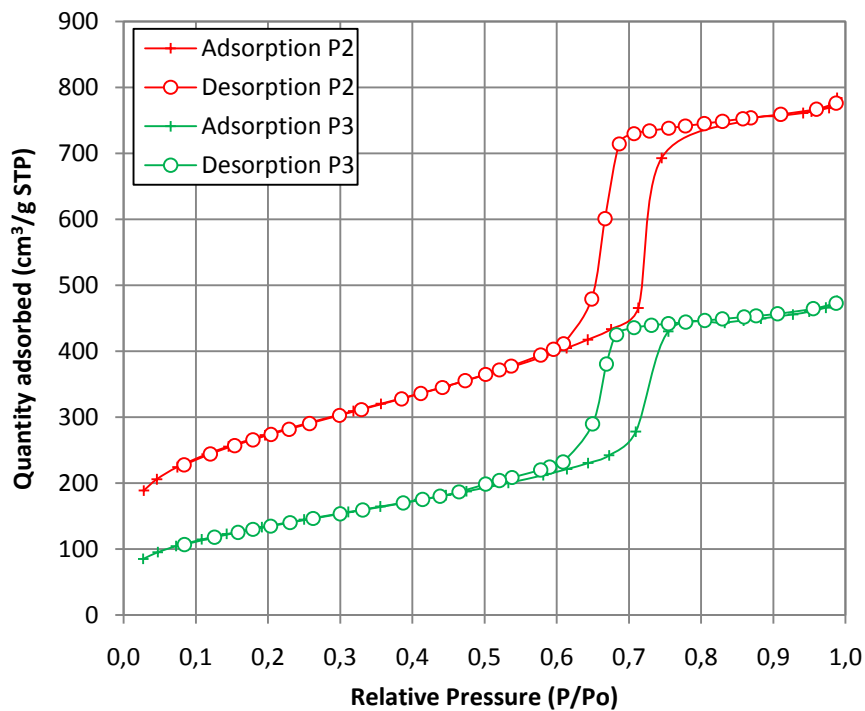
Figure 16. N$_2$-sorption for samples P2 and P3.

Table 1 shows that the adsorbed amount of N$_2$ in the material synthesised with 6 g of TEOS is much lower than the synthesised with 8.5 g. The surface area was drastically decreased in the second synthesis. Even so, both isotherms correspond to type IV, which means mesoporous material was obtained [31].

Table 1. N$_2$-sorption results for synthesis with P2 and P3.

	BET surface area [m^2/g]	Pore volume [cm^3/g]	Pore size [Å]
8,5 g TEOS	*985,8106*	*1,197606*	*48,5938*
6,0 g TEOS	*495,0711*	*0,729195*	*58,9164*

We can observe that reducing the surfactant/silica ratio the order of the pore structure inside the material is decreasing (see figure 17).
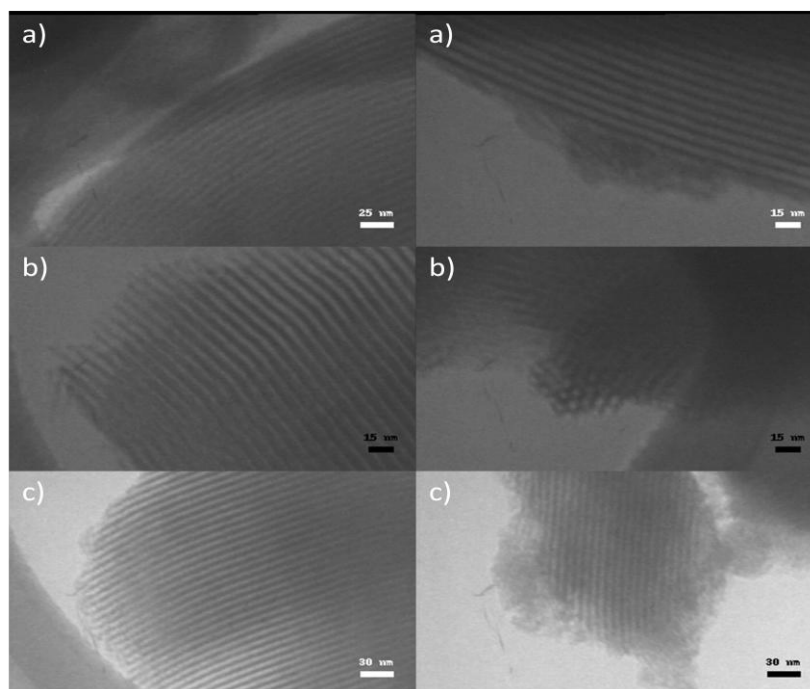
Figure 17. TEM images of silica particles a) P1, b) P2 and b) P3.

The Images on the TEM showed some amorphous silica in the second synthesis with some areas where no pattern is observed. Those areas may be due to the effect of the delution. Table 2 shows synthesis P1 and P2, where the water content is varied. And according to the particle size, no significant differences were observed in the TEM, so we could not get smaller particles increasing the amount of water.

Table 2. N$_2$-sorption results for P-series.

	TEOS [g]	Water [g]	BET surface area [m^2/g]	Pore volume [cm^3/g]	Pore size [Å]
P1	*8,5*	*30*	*843,7694*	*0,994751*	*47,1575*
P2	*8,5*	*100*	*985,8106*	*1,197606*	*48,5938*

It has been reported that the temperature during the aging process influence in the pore size [35, 36]. So synthesis *P1* was repeated but increasing the temperature of aging at 140°C (*P4*) and 150°C (*P5*) for 20 hours. According to the results shown in table 4 the

pore size was increased when increasing the temperature. The desired pore size in this study is around 90-100 Å and this was reached for P4 and P5.

Table 3. N$_2$-sorption results for P-series.

	TEOS [g]	Water [g]	BET surface area [m^2/g]	Pore volume [cm^3/g]	Pore size [Å]
P2	8,5	100	985,8106	1,197606	48,5938
P3	6,0	100	495,0711	0,729195	58,9164
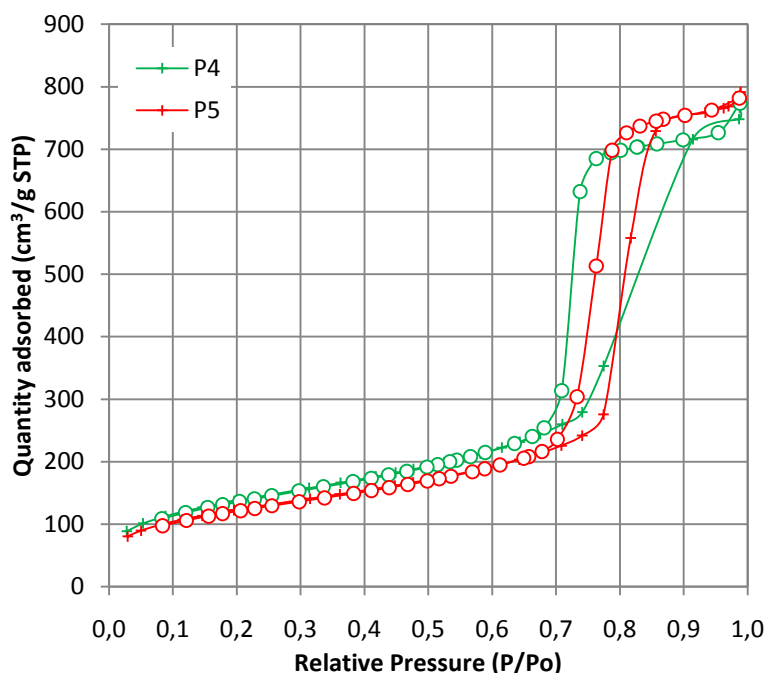
Figure 18. N$_2$-sorption isotherms for samples P4 and P5.

According to the figure 17 and 18, we can be sure about the dilution effect on this synthesis. Adding water the mesoorder is getting worse, some amorphous silica can be observed in the particles. In the figure 17 we can observe how the quantity absorbed is reduced. The reason is the order was getting worse. The less porous the material is, the less quantity of absorbed is.

Table 4. BET results for P-series.

	TEOS [g]	Water [g]	BET surface area [m^2/g]	Pore volume [cm^3/g]	Pore size [Å]
P1 (100°C)	8,5	30	843,7694	0,994751	47,1575
P4 (140°C)	8,5	30	502,2647	1,186326	94,4782
P5 (150°C)	8,5	30	448,6427	1,206143	107,5370

After the heat treatment at higher temperatures, the pore size reached was the ideal for the encapsulation of lipase. Then in this point we can conclude between the range 140-

150 °C we can get the optimum pore size for our purpose, lipase encapsulation. About the particle size, no lower sizes were reached with the dilution experiments, or with the addition on KCl to the initial mixture.

SAXS measurements (figure 19) show 5 Bragg peaks which means a really good mesoorder was obtained in the material P4 and P5. The distance between the Bragg peaks corresponds to a hexagonal pattern [26, 27].
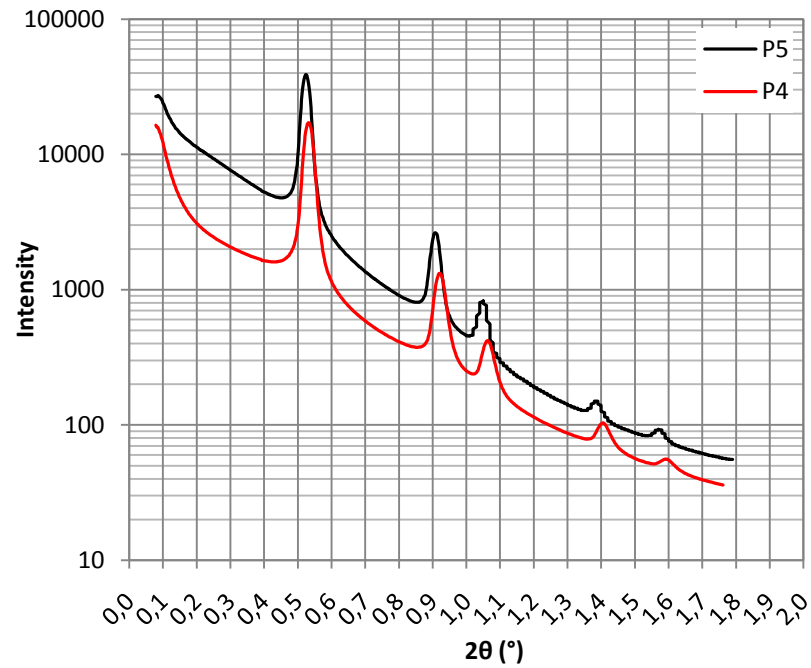
Figure 19. SAXS results for samples P4 and P5.
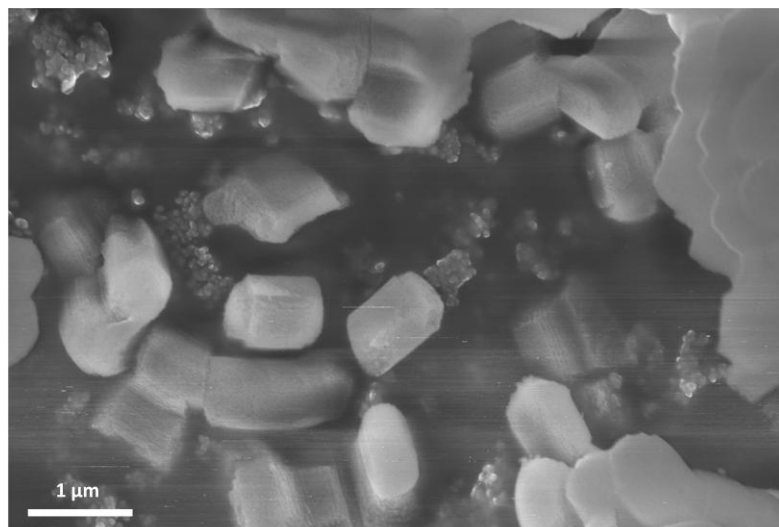
Image 1. SEM image for sample synthesised without KCl.
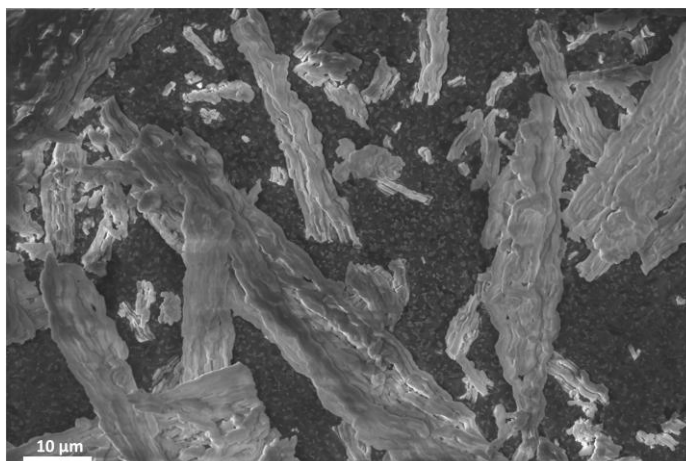
Image 2. SEM image for sample synthesised with 8g of KCl.

Comparing the two images (image 1 and 2) we can observe that the result is surprisingly opposite to that intended. On image 3 the form of one particle within the aggregate can be observed in detail. Images reveal that the particle size is around 1 µm as we saw previously in the TEM images. Probably these aggregates are due to the continuous and vigorous stirring applied during the reaction time. Notice that in the previous reports this synthesis took place under static conditions [32].
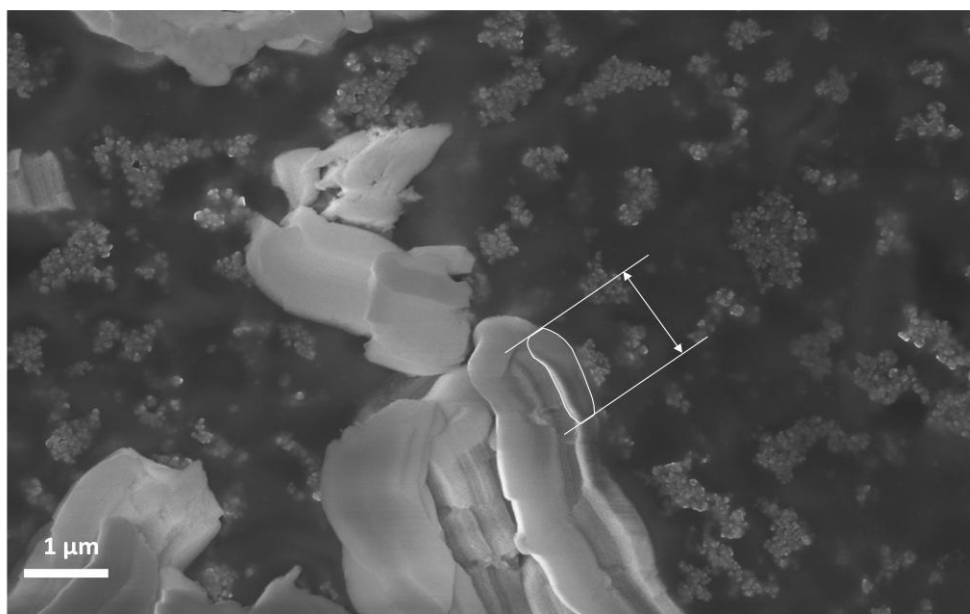
Image 3. SEM image for a sample prepared with 8 g of KCl. A particle within the aggregate is marked.

5.2. Synthesis II

In the second synthesis we worked with a sodium silicate solution [SiO_2:Na_2O] instead of the TEOS. Smaller particle sizes were reported in previous studies using this synthesis [37, 38]. Silica is soluble in water and is strongly dependent on pH. At high pH silica become highly stable in water solutions (15 – 35 wt.%)[39]. Before the reaction, the silica solution has to pass through strong ion-exchange resin in order to get an acidic solution. This ion-exchange resin changes sodium cations for protons, lowering the pH until values around 3 (see figure 20). After the ion exchange the reactions took place immediately.

$Na_2O : SiO_2$
Water glass solution

Amberjet 1500H

Pluronic P123 solution
Surfactant template

$SiO_2 + H^+$
Acidic silica solution

Strong ion-exchange resin
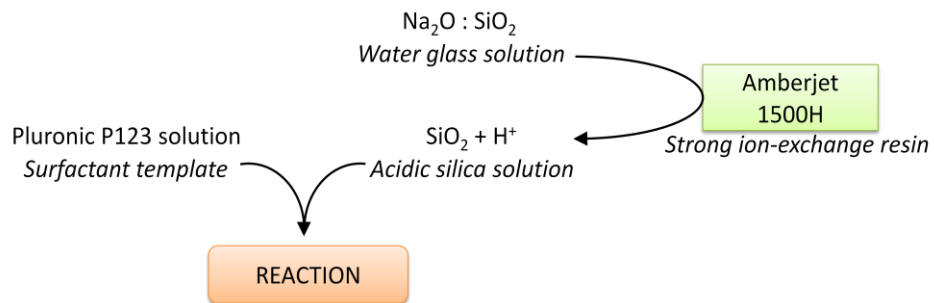
REACTION

Figure 20. Scheme of reaction for synthesis II.

According to previous studies [36, 40], we knew that the lower amount of silica and the lower pH value, the lower particle size could be reached. So we chose different surfactant/silica weigh ratios (1,0/1,5/2,0) and observed the effect of the dilution on the particle size.

For the determination of the particle size, dynamic light scattering was used (table 5) as well as TEM (figure 27).

Table 5. Conditions used and results observed in the A-series synthesis.

	Surf./Sil.	Water /Sil.	pH	Particle size[nm]
A1	1,00	50,49	2,96	239,3
A2	1,00	75,39	2,96	219,6
A3	1,00	100,41	2,96	222,0
A4	1,00	125,57	2,96	183,7
A5	1,00	150,59	2,96	178,0
A6	1,00	175,55	2,96	176,2
A7	1,01	197,47	2,96	169,3
A8	1,00	249,91	2,96	160,0
A9	1,00	301,05	2,96	155,3

In figure 21 we can observe clearly a trend, increasing the water/silica ratio the particle size becomes smaller.
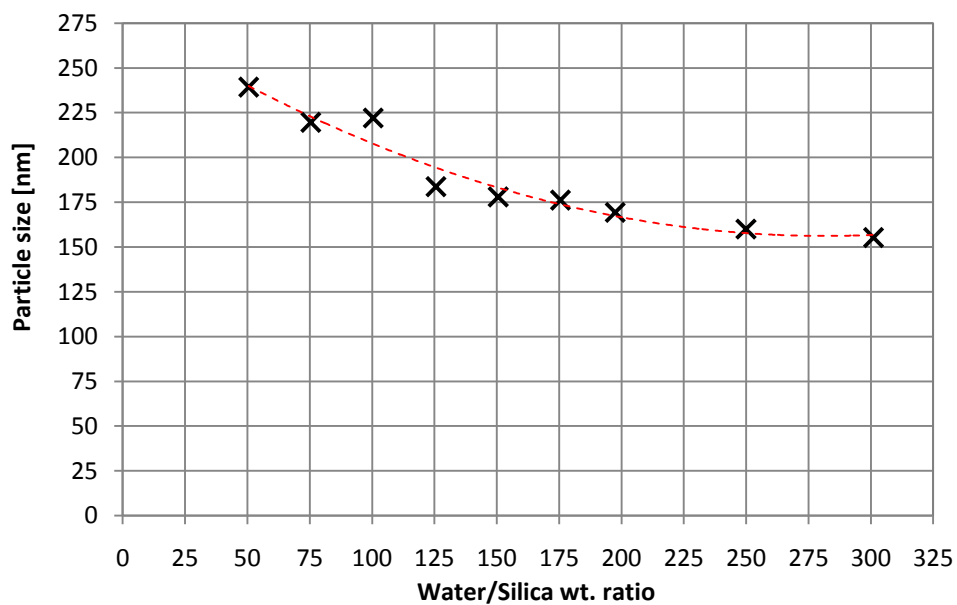
Figure 21. Graph of the particle size in front water/silica ratio for A-series Synthesis.

The results for the synthesis with 1.5 and 2.0 surfactant/silica ratio were is shown in table 6 and 7 respectively.

Table 6. Results for B-series synthesis.

	Surf./Sil.	Water /Sil.	pH	Particle size[nm]
B1	1,50	51,21	3,35	271,50
B2	1,50	74,95	3,35	190,00
B3	1,50	100,15	3,35	200,80
B4	1,50	124,89	3,35	182,80
B5	1,50	149,98	3,35	193,80
B6	1,50	174,67	3,35	179,20
B7	1,51	200,20	3,35	151,30
B8	1,49	224,49	3,35	147,90
B9	1,49	248,21	3,35	142,60
B10	1,50	275,06	3,35	133,70
B11	1,50	300,38	3,35	136,50
B12	1,49	323,40	3,35	123,20
B13	1,49	348,18	3,35	119,10

Table 7. Results for C-series synthesis.

	Surf./Sil.	Water /Sil.	pH	Particle size[nm]
C1	1,99	66,78	3,18	595,9
C2	2,00	75,03	3,18	354,5
C3	2,00	100,04	3,18	236,5
C4	2,00	124,91	3,18	197,7
C5	2,00	150,12	3,18	175,5
C6	2,00	175,13	3,18	172,1
C7	2,00	200,04	3,18	164,5
C8	2,01	226,19	3,18	155,8
C9	1,97	247,34	3,18	154,5
C10	1,97	271,87	3,18	145,7
C11	1,99	297,71	3,18	145,2

If we plot all the results in the same graphic (figure 22) we can see the trend on the particle size. With more amount of water the particle size is reduced. That is due to we are creating more amount of nucleation cores. After repeating several times these synthesises we noticed that the lower surfactant/silica ratio is, the lower particles size is reached. Although the differences were not significant.
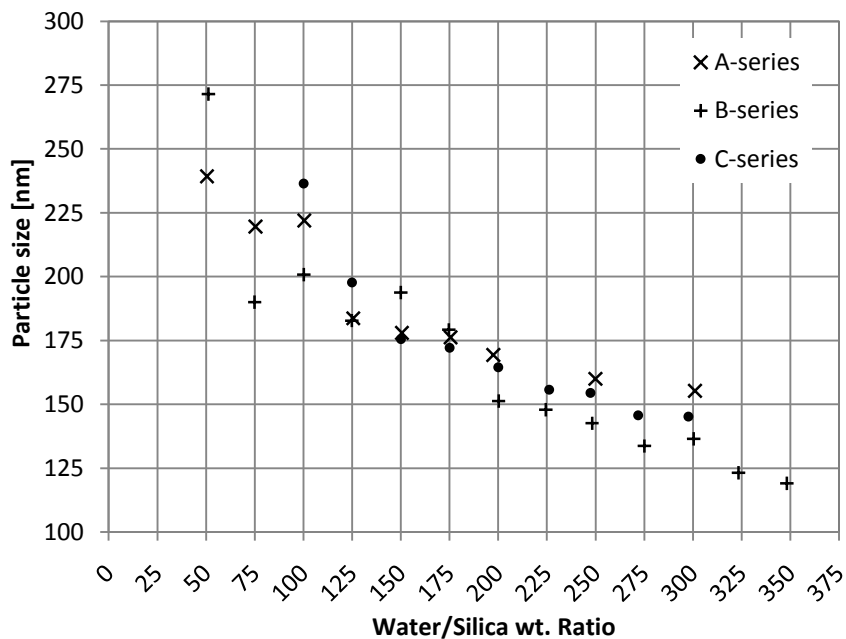
Figure 22. Plot of A, B and C-Series.

According to the previous results, we tried to work with lower surfactant/silica ratios. 0,8 was chosen to observe the particle size. Table 9 shows the results.

Table 8. Results for the D-series.

	Surf./Sil.	Water /Sil.	pH	Particle size[nm]
D1	0,80	50,05	3,20	235,10
D2	0,80	74,86	3,20	183,70
D3	0,80	100,04	3,20	165,20
D4	0,80	124,87	3,20	165,40
D5	0,80	150,19	3,20	166,80
D6	0,80	174,71	3,20	155,90
D7	0,79	198,59	3,20	148,40
D8	0,80	224,04	3,20	153,30
D9	0,79	247,70	3,20	141,10
D10	0,80	275,71	3,20	146,70
D11	0,80	300,30	3,20	140,70
D12	0,80	326,12	3,20	142,60
D13	0,80	350,58	3,20	135,00

We can also compare the results between D-series and A-series due to their proximity on their surfactant/silica ratio. The figure 23 shows the plot between both syntheses.
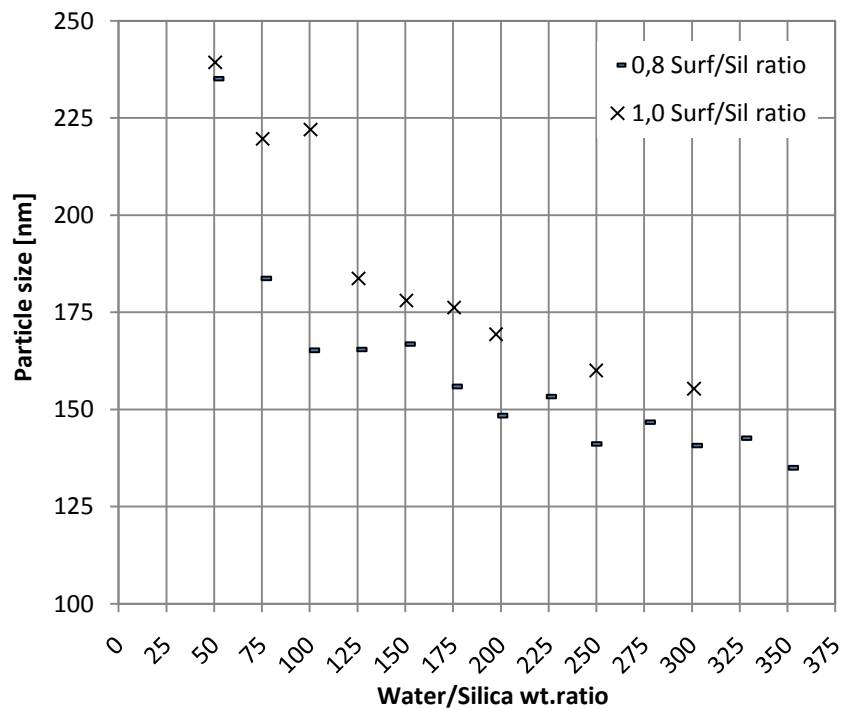
Figure 23. Variation of the particle size in relation on the water/silica ratio.

We can corroborate that the effect of the dilution makes smaller the particle size, and it is observed reduction on the particle size when the water/silica ratio is been decreased. To see the effect on the particle size when the surfactant/silica ratio is being altered we

can observe the previous plots. Adjusting one line trend between the ratios 100 and 200 on each series we can see that the slope of this line is more pronounced when the surfactant/silica ratio is higher. With this we can deduce that the reduction of surfactant/silica ratio decreases the particle size. The figure 25 shows how the trend becomes steeper when the ratio is increased. Of course we cannot that the particle size has a linear trend with the water/surfactant ratio, but it helps to prognosticate the effect with a supposed variation of surfactant/silica ratio.
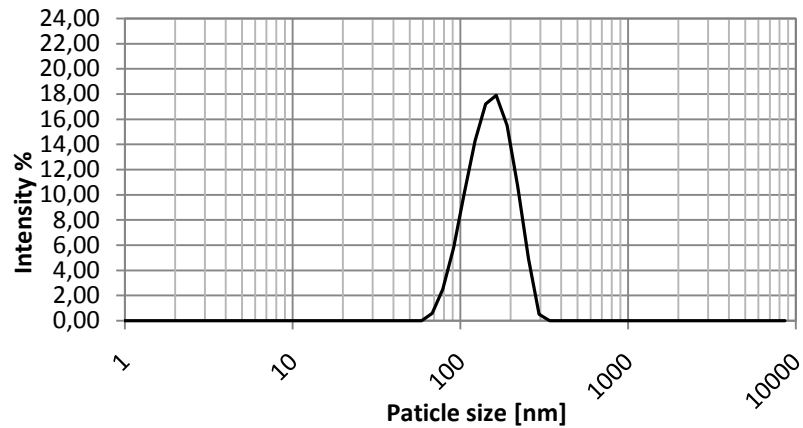
Figure 24. Particle size distribution for sample B9.
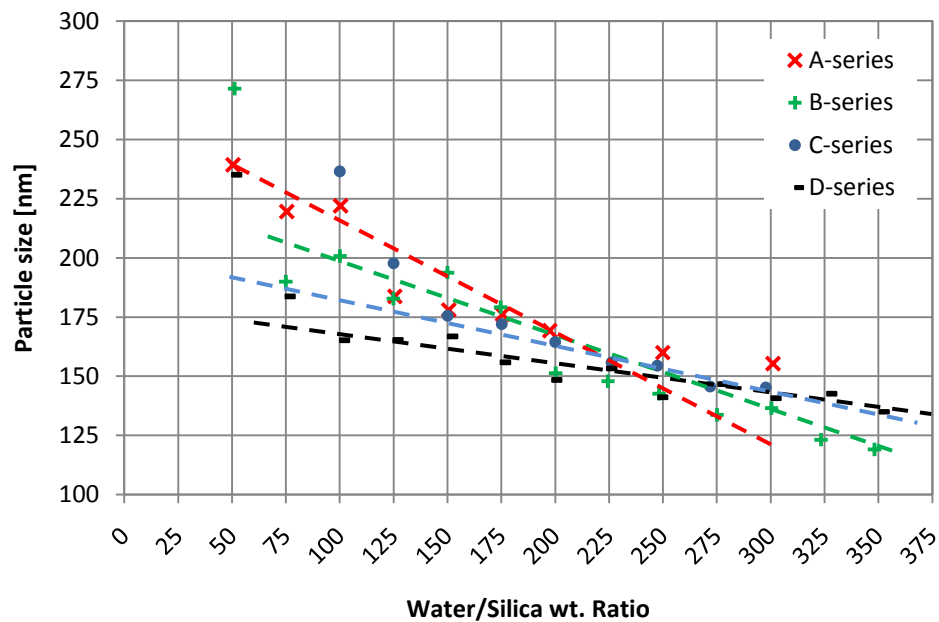
Figure 25. Trend on reduction.

In order to determine a clear trend, different values in the surfactant/silica ratio are shown in the next table.

Table 9. Results for E-series.

	Surf./Sil.	Water /Sil.	pH	Particle size[nm]
E1	1,00	199,4	2,88	206,3
E2	1,25	199,4	2,88	221,8
E3	1,50	199,9	2,88	229,4
E4	1,75	200,3	2,88	251,9
E5	2,00	200,0	2,88	236,2
E6	2,99	199,1	2,88	208,2

Despite the last two points show a reduction in the particle size, a trend on increasing the particle size can be observed as seen in figure 26. After repeating this experiment several times, the trend is clearly to increase the particle size.
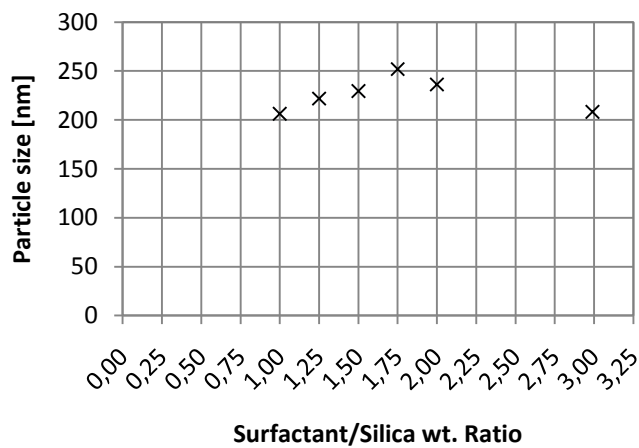
Figure 26. Graphic representation of the E-series.
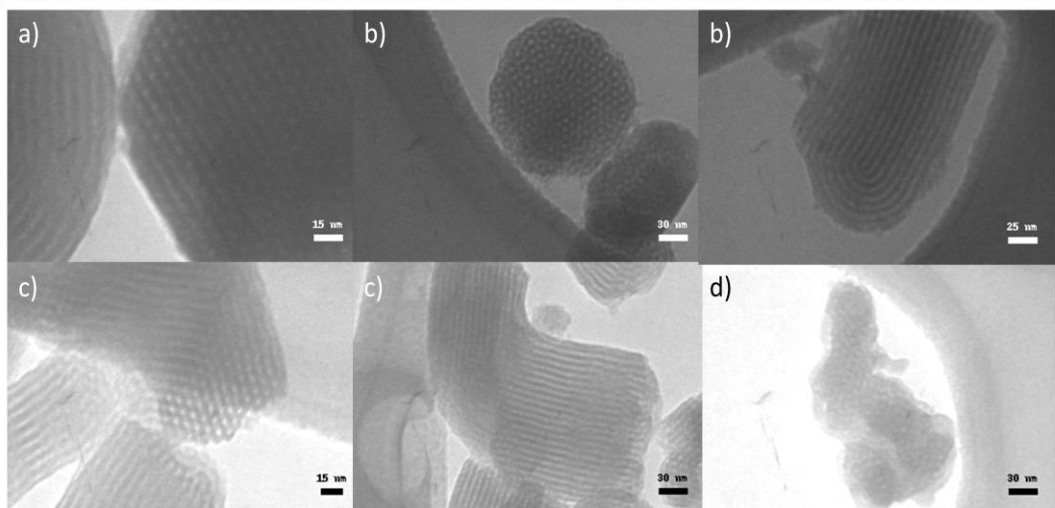
Figure 27. TEM images for samples a) E2, b) E3, c) E5 and d)E6.

According to the figure 26 we can observe a good mesostructure but we can find diverse shapes of particles. In the sample *E6* presence of gellation was observed after some hours.

After observing the particles with the TEM a lot of varieties of particle size and shapes were observed. With this synthesis has been noticed that is really difficult to repeat, it is hard to handle. In the figure 27 can be observed the variety of shapes that could be reached with this synthesis. Figure 27 shows different shapes of particles, all of them are spherical but particles from 60 nm to more than 200 nm can be observed. A large range of sizes were observed in the TEM. The particle size distribution obtained by using the DLS was showed before (see figure 24).

Also, the figure 28 shows the pore structure of the particles. A regular pore size can be observed in the picture. However, the mesorder is not hexagonal. One can sense that the structure is intented to be hexagonal, but is not. This is in conflict with figure 27, where a good order was observed.

Figure 28. TEM pictures of the synthesis B7.

Looking at the pore size low values were achieved, always between 30 Å and 55 Å. In accordance with the BET results, the particles are really porous, but in the other hand, according to the TEM images, the structure is not completely hexagonal.
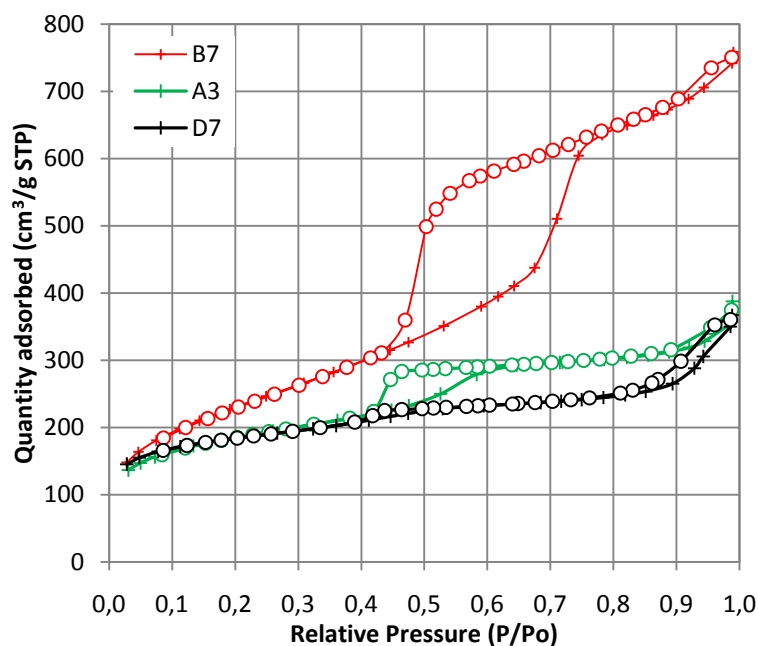
Figure 29. N$_2$-sorption for samples B7(surf/sil = 1.50, w/sil = 200), A3(surf/sil = 1, w/sil = 100) and D7(surf/sil = 0.8, w/sil = 200).

The BET results are showed in the table below. The isotherms observed are type IV, which means mesoporous material was obtained. About the hysteresis loop in the sample D7 is type H4, which is associated with narrow slit-like pores [31]. That is a symptom of not cylindrical pores in the particle.

Table 10. BET results for synthesis II.

	Surfactant/ Silica	Water/ Silica	BET surface area [m^2/g]	Pore volume [cm^3/g]	Pore size [Å]
A3	1,00	100,41	657,5297	0,9873340	34,84
B7	1,51	200,20	641,8722	0,9700242	192,35
E6	2,99	199,10	850,9402	0,9657679	202,93
E7	3,00	295,20	742,9139	0,9873951	38,06
D7	0,79	198,59	638,1659	0,9867869	34,67

The BET results show some incorrect data such the pore size for samples *B7* and *E6*. The pores can be observed in the figure 30 and they do not fit with the BET results. They seem to be quite narrow, between values of 30 Å or 40 Å. As said in the introduction, the pores with a size around 90 Å are the most interesting for encapsulating lipase.

A new series of experiments were done in order to increase the pore size by adding a new stage in the synthesis procedure.
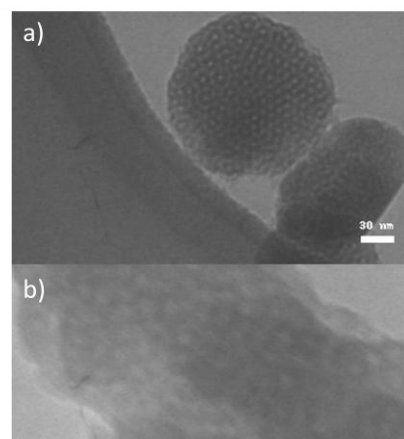
Figure 30. TEM images for samples a) B7 and b) E6

SAXS measurements only show only one Bragg peak for the syntheses 0.8 (D7)and 1.0 (A7) surfactant/silica ratio, both with 200 water/silica ratio. But the SAXS measurement for synthesis A3 shows a second peak slightly. This second peak, represented in the figure below as a dotted red line corresponds to the third peak for the hexagonal pattern [26, 27].
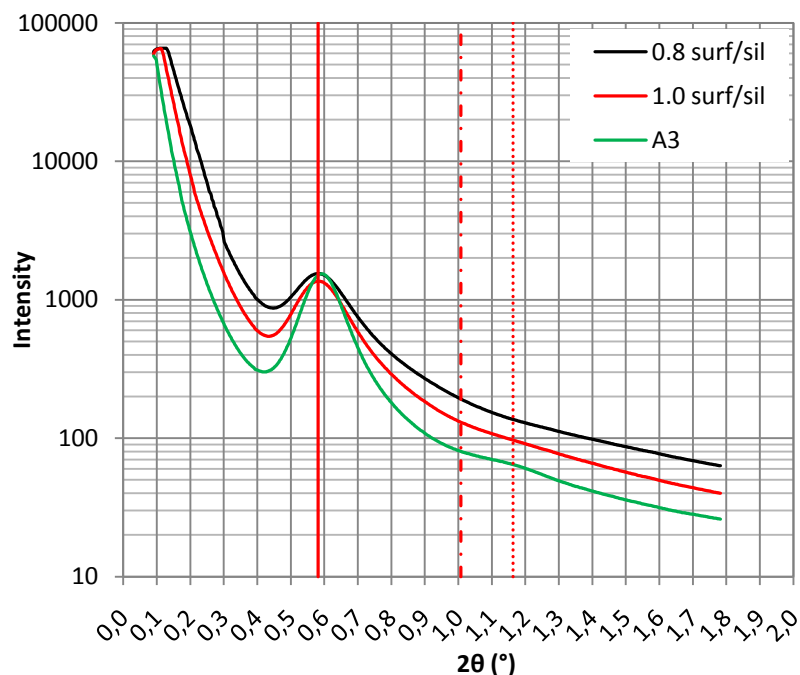
Figure 33. SAXS results.

The SAXS results plus the TEM images told us that even mesoporous material was obtained, this was not completely hexagonal. As seen in the TEM pictures, one can sense an hexagonal order, but this is not well defined.

This new stage is the aging of the sample in an autoclave at different temperatures for 24 hours. As is reported in previous studies [35, 36], the pore size can be modified by aging the sample at different temperatures. The table below show the results for this new experiment.

Table 6. Results for the F-series.

	Surfactant/Silica	Water/ Silica	Temp. [°C]	BET surface area [m²/g]	Pore volume [cm³/g]	Pore size [Å]
F1	1,00	200,00	Room temp	839,8314	0,988984	55,13
F2	1,00	200,00	140	511,7985	0,990683	37,14
F3	1,00	200,00	180	496,8009	0,993845	92,55

The hysteresis loop for the sample *F3* corresponds to type H3. These types of hysteresis loops owe their form to presence of aggregates.
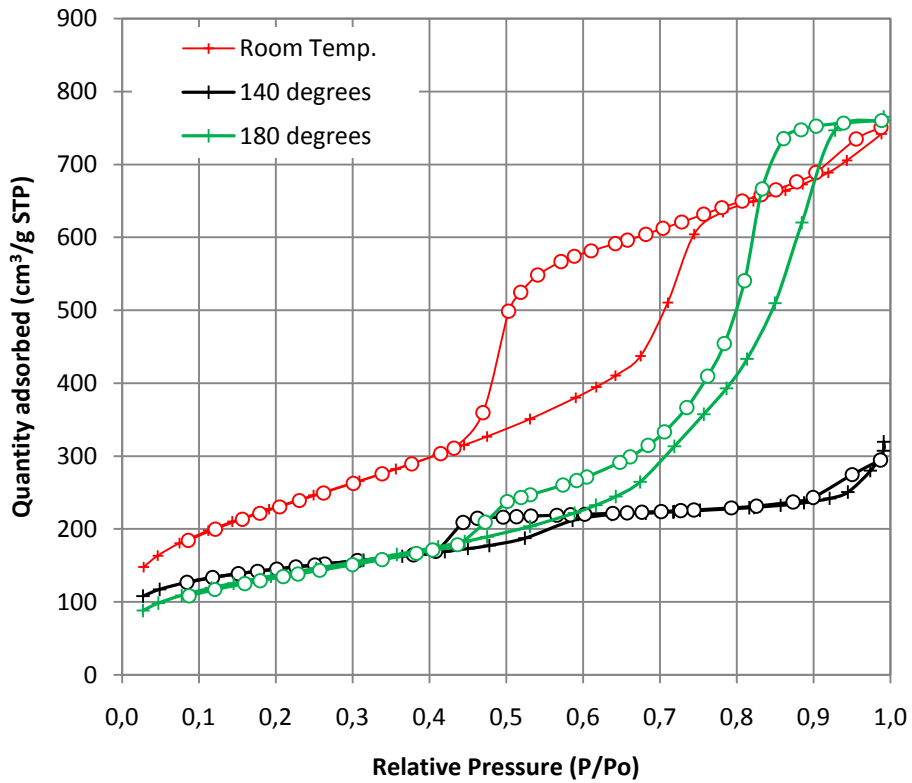
Figure 31. N2-sorption for F-series.

Pictures on the TEM showed a large variety of particle sizes. For the synthesis at room temperature the images were as seen in figure 28. In the other hand, in the material synthesized at 140 °C, the images showed the same pattern of size plus some smaller particles. Sizes reached values of 50 nm. Figure 32 shows the variety of sizes achieved in this stage.
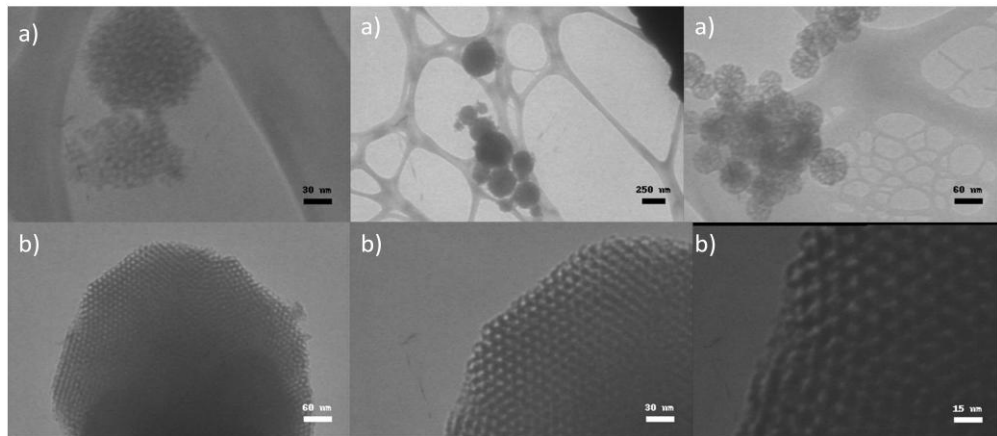
Figure 32. TEM pictures for synthesis a) F2 and b) F3.

5.3. Synthesis III

Synthesis III is based in a novel work reported by *K.Okuyama et al.* [42]. They used a cationic surfactant to create a micellar system, one emulsion between water and octane as non polar support. TEOS is used as a silica source, and polystyrene as mesostructural template. Both will move inside the octane droplet because they are hydrophobic. L-lysine is used as a limiter of particle growth [42]. Also N_2H_4 and ammonia can be used as a catalyst and as limiter of particle growth, but it has been reported that larger particles were obtained, larger than 100 nm [42-45]. The effect of l-lysine plus the wall of the micelle, provide particle sizes really small which is the main objective of the work. As starter for the styrene polymerization the amino acid *AIBA (2,2'-Azobis (2-methylpropianoamidine))* was used. These silica mesoporous materials are also known as *Hiroshima Mesoporous Materials (HMM)*.
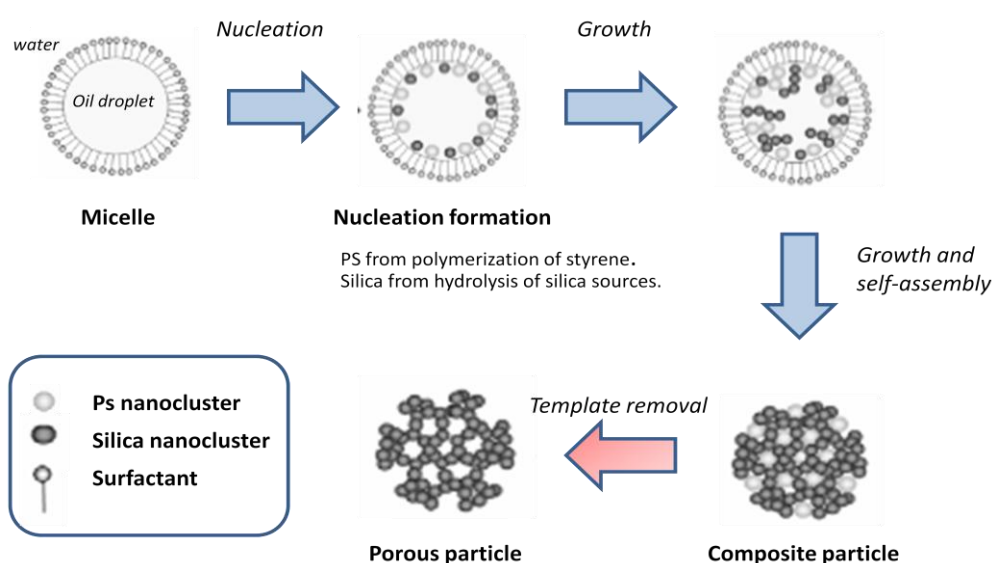
Figure 34. Reaction mechanism for a silica nanoparticle.

In other papers was reported that the amount of octane affects on the particle size, and the pore size is affected by the amount of styrene added [42].

Table 7. Results for the G-series. Styrene and AIBA are expressed in mg per total volume.

	Octane/ Water	Styrene [mg/l]	AIBA [mg/l]	BET surface area [m²/g]	Pore volume [cm³/g]	Pore size [Å]	Particle size [nm]
G1	0,20	20,11	0,85	479,2920	0,979186	106,16	55
G2	0,32	8,93	0,85	559,7754	0,986269	83,03	70
G3	0,32	20,24	0,85	471,5695	0,985576	82,45	55
G4	0,32	30,13	0,85	502,3602	0,979484	89,78	50
G5	0,32	39,92	0,86	499,2527	0,986345	87,31	65

No trend can be observed on the pore size and in the particle size. We could not increase the amount of styrene because with amounts superior than 40 mg/l there was

a lot of problems in handle the material, so we chose 40 mg/l as a limit value. The particle size was measured by DLS but not logical values were obtained. Thus, the *Feret method* was used to determine the particle size. Pore size was determined by N_2-sorption just we did before.

Images observed on TEM, does not show a significant difference between the particles (fig. 35). The pore structure of course is not hexagonal, but the pore size seems to be really appropriate for the encapsulation of lipase.
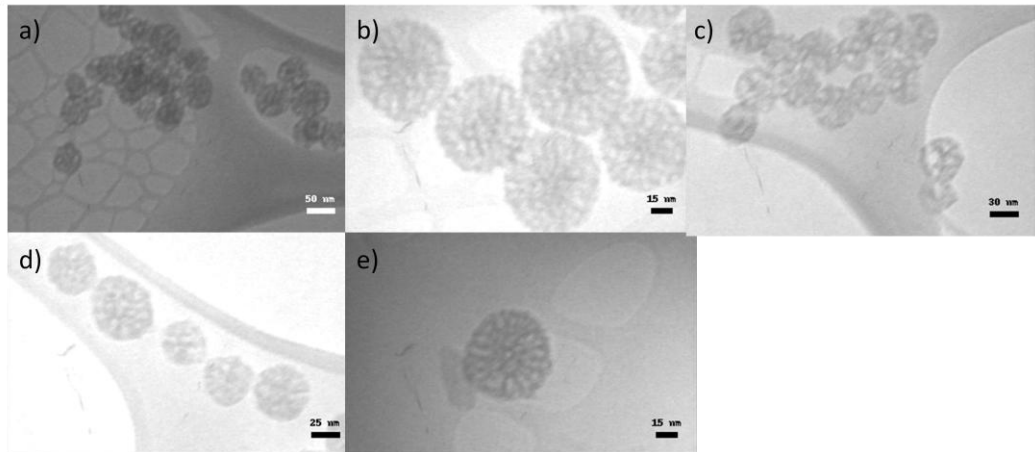
Figure 35. TEM Images forr samples a) G1, b) G2, c) G3, d) G4 and e) G5.

The pores seems to be radial oriented and according to the images and the BET surface area we can assume that the particles has a closed mesopore channel. The sorption isotherms show a mesoporous material as we can see (fig. 36).
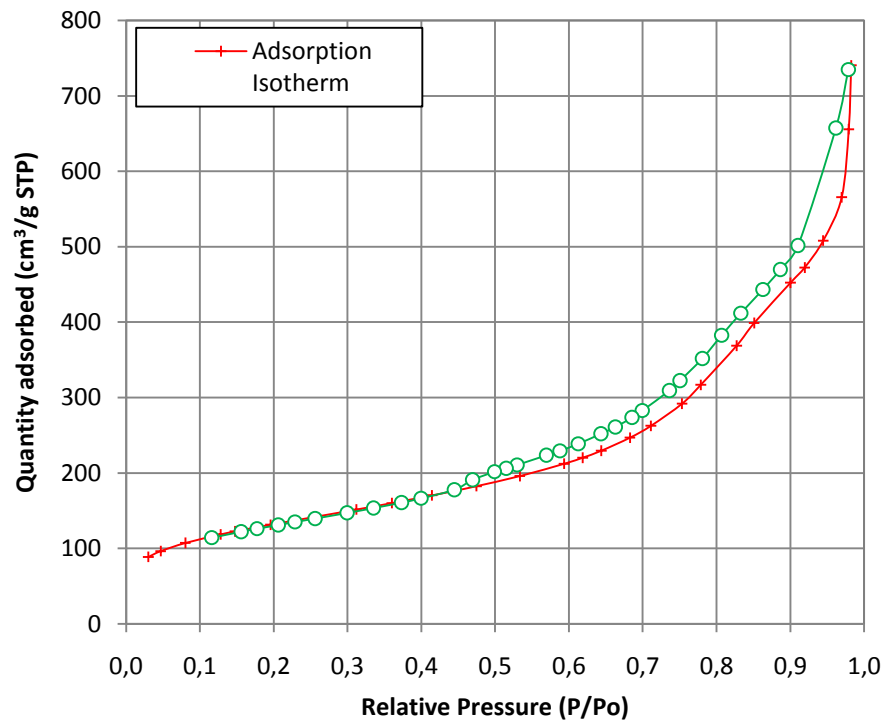
Figure 36. N_2 – sorption for sample G1.

The hysteresis loop is the type H3. Does not shows a limit in the adsorption at high p/p°, this type of hysteresis is shown in presence of aggregates and slit-shaped pores. The TEM images confirm the last supposition, non cylindrical pores are observed in the pictures, they are more elongated. So, slit-shaped pores are achieved with this new synthesis. About the mesoorder, using polystyrene as a template we got a random network. Observing the SAXS results not structure can be observed. We can sense some peaks, but they are not corresponding to the hexagonal pattern.
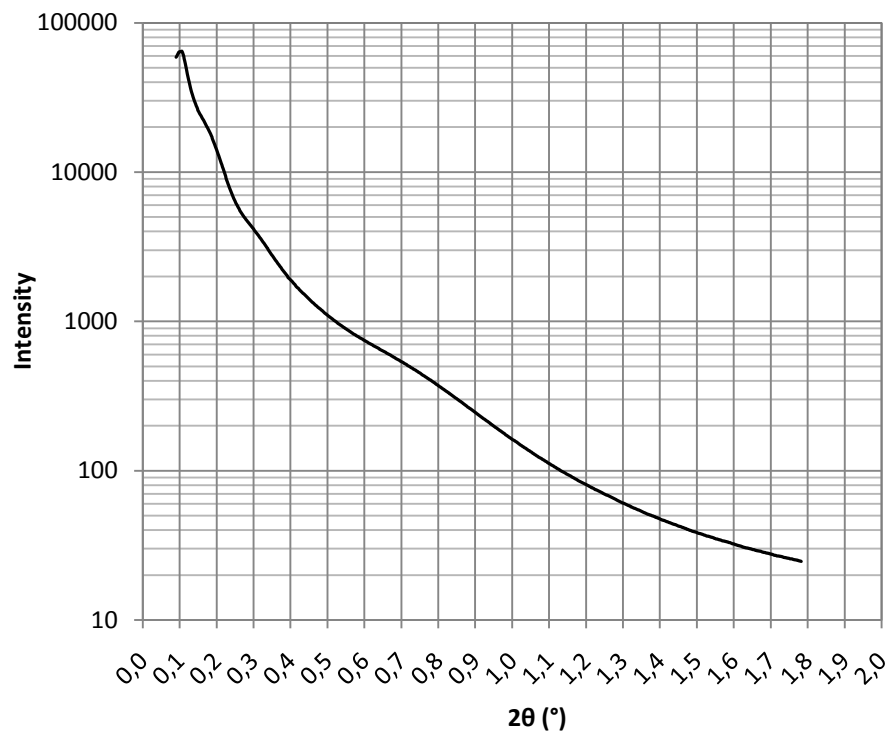
Figure 37. SAXS Results for sample G4.

At values 0.2, 0.3 and 0.7 for 2θ, slightly peaks can be observed, but they not correspond to the hexagonal pattern described in the literature [26, 27]. But it should not be important as long as the material was porous and moreover, with the optimum pore size described for the lipase immobilization. The slit-shape of the pores is more worrying than the pore structure (for this case). No data about lipase immobilization in this material has been reported before.
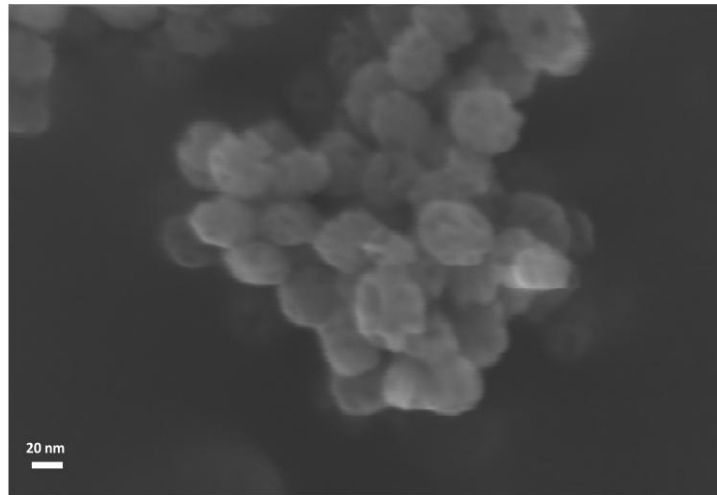
Image 4. SEM image for particles synthesised on synthesis III.

SEM image shows really spherical particles, with an homogenius size. The pores can be observed in the picture. As the SAXS results said, there is no order in the porous structure, even so a high porous material was obtained.

5.4. Synthesis IV

In this last chapter the previous synthesis was simplified according to the paper reported by *X.Bao et al* [46]. The idea is create an emulsion using water and octane as a hydrophobic supporter and as a swelling agent. Previous studies have being made with different hydrophobic supports [47]. Octane was selected from hexane, heptane , nonane and decane because a proper pore size was reported [46-49]. NH_4F was used as a catalyst for the TEOS hydrolysis.

Different amounts of octane were chosen in order to study the effect in the particle size according to the previous synthesis [46]. One control experiment was designed with 8 g, 12 g and 16 g of octane. The table below show the results for this synthesises.

Table 8. N_2-sorption results for H-series.

	TEOS [g]	Octane [g]	BET surface area [m²/g]	Pore volume [cm³/g]	Pore size [Å]
H1	4,0	8,0	216,1025	0,987025	97,23
H2	4,0	12,0	254,6613	0,987782	255,71
H3	4,0	16,0	232,9075	0,988346	125,80
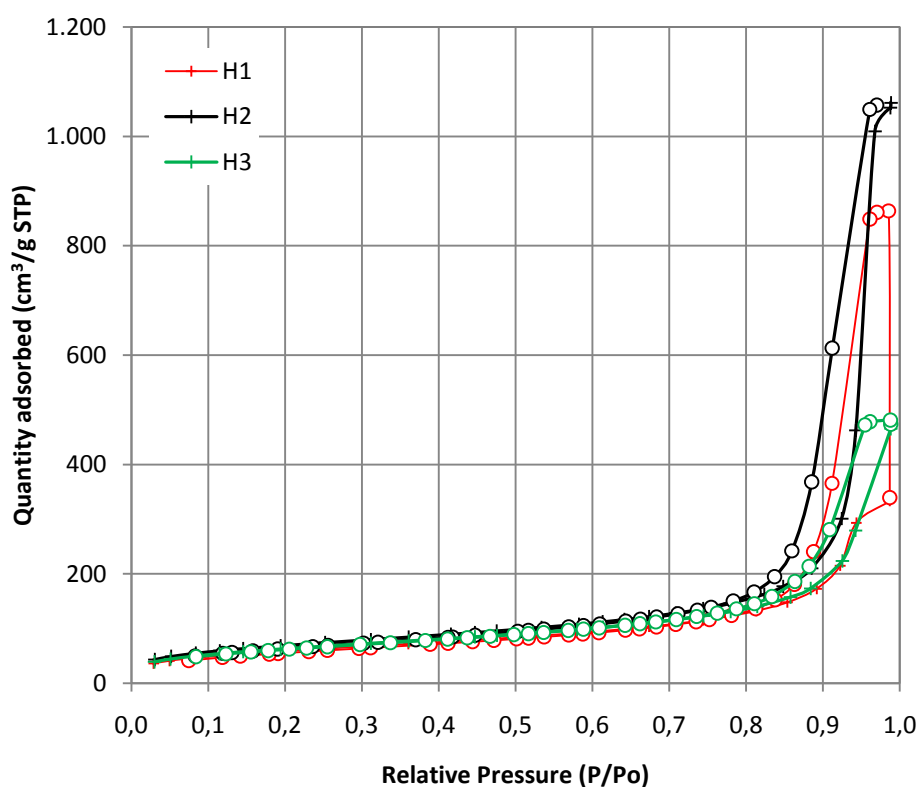
Figure 38. N2-sorption plot for H-series.

The N_2-results show a porous material but with a really bad order. A type-IV isotherm can be observed, but the specific area is pretty low. Adsorption only happens at high

values of p/p°. Nothing related with the 600 m^2/g reported in previous studies [46]. TEM images show amorphous silica with some random pore, without following any kind of pattern in the mesostructure (fig. 40). The synthesis was repeated several times in order to get a proper material according to the papers found in the bibliography, but no success was achieved. Only amorphous silica was synthesized with random pores in the structure without following a defined pattern. SAXS measurements show amorphous non-porous material for the all synthesis realized.
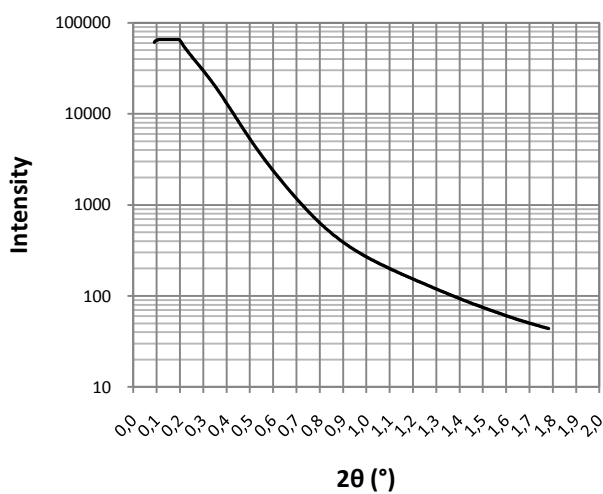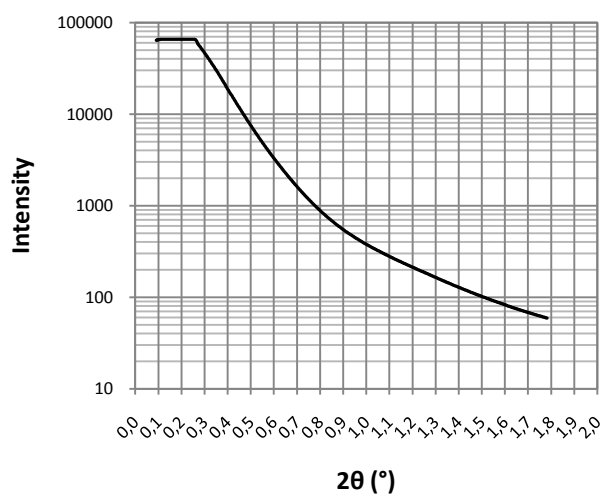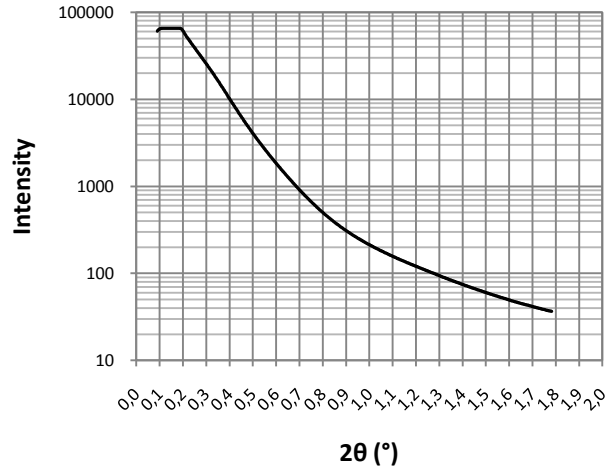
Figure 39. SAXS results for samples H1, H2 and H3.

These results could be explained for the following explanation. TEOS as a non-polar spices remains in the octane droplet during the reaction time while the surfactant remains in the aqueous phase. This synthesis took place in acid conditions where the block copolymer generally is more hydrophilic [4]. In this manner there is no interaction between the liquid crystal template and the silica source. As a consequence, amorphous silica is obtained.
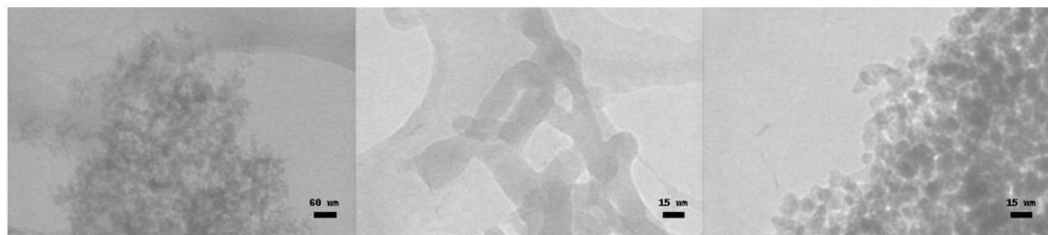
Figure 40. TEM Images for synthesis IV.

5.5. Conclusion

According to all the results obtained in this work, now we can compare each one. The next table gather the most promising samples achieved during this work.

Table 9. Optimal synthesis results.

	BET surface area [m^2/g]	Pore volume [cm^3/g]	Pore size [Å]	Particle size [nm]
P4	502,2647	1,186326	94,48	~1 μm
P5	448,6427	1,206143	107,54	~1 μm
F3	496,8009	0,010331	92,55	169,3
G1	479,2920	0,979186	106,16	55
G4	502,3602	0,979484	89,78	50

Of course the most interesting material under the point of view of particle size, are the materials achieved using the synthesis number III. The smallest particles were reached and with a really uniform particle size as seen in the TEM images. Moreover, the synthesis is quite easy to control and reproduce. But this synthesis presents one inconvenient, as seen in chapter 4.3, the pore shape is not spherical at all. The pores are slit-shaped, that maybe is not good at all for encapsulation of lipase. Loading capacity in these particles should be checked and compared with hexagonal material.
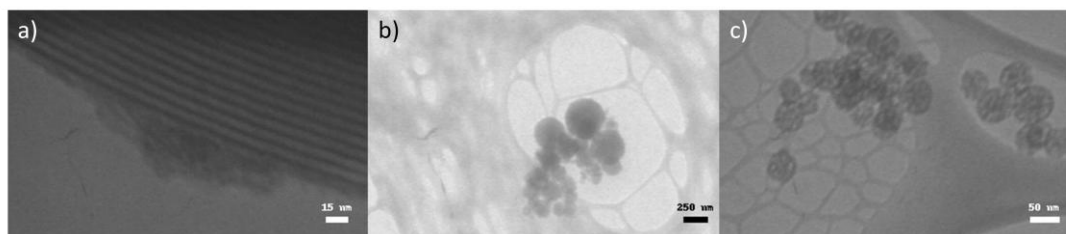
Figure 41. TEM images for a) P4, b) F3, c) G1.

Synthesis F3 described in the chapter 4.2 present more varieties of shapes and a wide distribution in the particle size. Comparing synthesis II with synthesis III, in the first one more different shapes and sizes were found. This one is really hard to repeat with the same results, which means that is really difficult to control. Furthermore, this synthesis is probably the most tricky to work with of all synthesises described in this study. When adjustment of the pore size was done, the pore shape also was altered. According to the BET results, as in the synthesis III, the pores became more slit-shaped than spherical. But observing the figure 42, we can observe a really good shape of the pores, completely cylindrical. Also a not defined spherical form could be observed in the figure 42. Lipase loading in both materials has not been done yet. Last synthesis, described on chapter 4.4 is not promising at all. The results obtained show amorphous silica with the presence of some random pores without any kind of pattern. Referring to synthesis I the effect of the dilution only increased the amount of amorphous silica without reduction in the particle size. In the other hand, the hexagonal pattern was really good as seen in the

SAXS analysis and the pore shape was cylindrical, according the TEM images and N$_2$-sorption plots.
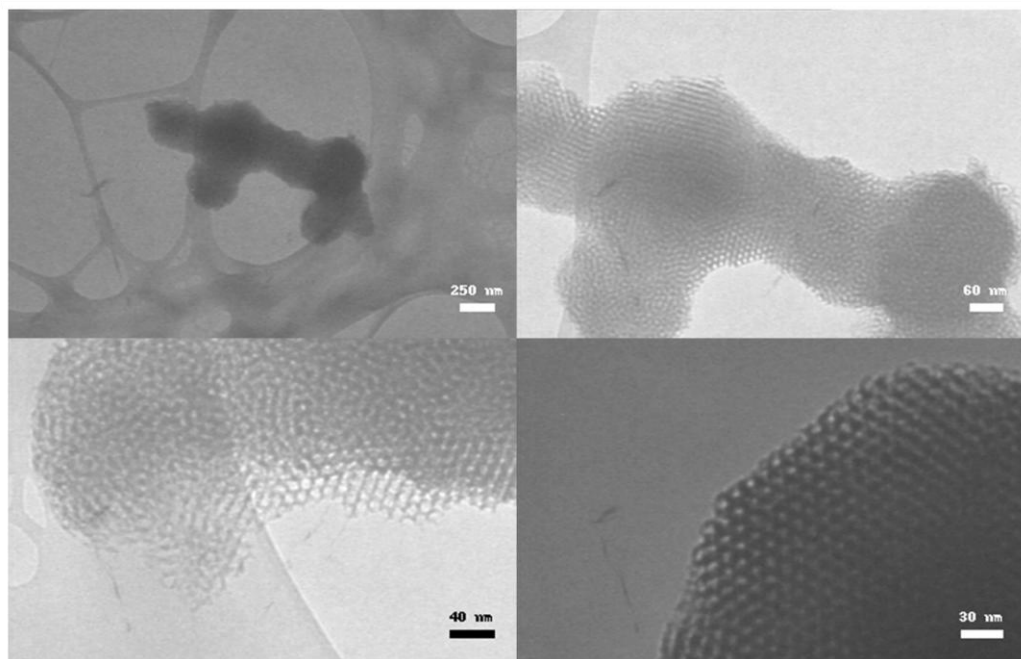
Figure 42. TEM images for sample F3 (synthesised at 180°C).

6. SUMMARY

In this project we were focused in getting the smallest particles size possible always trying to keep the pore size and structure constant. In order to be able to achieve the objective described, we had to walkthrough different synthesis found in an extensive literature. This way, different silica sources, different types of templates and different conditions of reaction were tried. Finally all the settings for each synthesis were described to be able to get the smaller particle possible. Synthesis III (*Hiroshima Mesoporous Materials*) has showed the most promising results. Really small particles can be obtained using this novel synthesis. Due to the results and their simplicity and its ease to repeat the results, we could say it is the best choice for enzyme encapsulation. Other synthesis, specially synthesis II which small particles were also obtained, are more difficult to control and reproduce the results, or not real small particles were reached (such synthesis I). Once the parameters were adjusted, as an outlook, the immobilization of lipase should be tried on the different materials and report if there is any influence in the encapsulation due to the deformation showed by the pores. Slit-shaped pores could hinder the encapsulation process.

7. ACKNOWLEDGE

I would like to express my sincere thanks to all those people who helped me during the performance of this thesis work. First of all to Chalmers University of Technology for give me the opportunity to join them and University of Barcelona for training me as a chemical engineer.

Special thanks to the professor Krister Holmberg, for all his support and help, and for guiding me through the world of silica; to Hanna Gustafsson who was my supervisor in this work.

Andreas Sundblom for all his help.

Ann Jakobsson, for helping to solve all my paper problems.

To all my friends in the department, especially to the people from the master student's room for all the good moments and for creating a funny and warm working atmosphere.

To Jaume Puigventós for introducing me into the world of chemistry when I was just a child.

I would like to mention all my mates and coaches from Göteborg Sim, for help me to "disconnect" and give the chance to travel around Sweden with them.

Finally, to my parents for encourage me day by day and support me on any situation.

8. REFERENCES

[1] *http://www.ipt.arc.nasa.gov/nanotechnology.html*
[2] M.A. Van Hove*, Catal. Today* 113 (**2006**), 113.
[3] X.Hu, S.Spada, S.White, S.Hudson, E.Magner, J.G.Wall, *J. Phys. Chem*. 110 (**2006**), 18703.
[4] Y.Wan, D.Zhao, *Chem. Reviews* 107 (**2006**), 2821.
[5] S.Hudson, J.Cooney, E.Magner, *Angew. Chem. Int. Ed.* 47 (**2008**) 8582.
[6] C-Y.Chen, S.L.Burkett, H-L Li, M.E.Davis, *microporous materials* 2 (**1993**), 27.
[7] J.s.Beck, J.C.Vartuli, W.J.Roth, M.E.Leonowicz, C.T.Kresge, K.D.Schmitt, C.T-W.Che, D.H.Olsson, E.W.Sheppard, S.B.McCullen, J.B.Higgins, J.L.Schlenker, *J. Am. Chem. Soc.* 114 (**1992**), 10834.
[8] C.T.Kresge, M.E.Leonowicz, W.J.Roth, J.C.Vartuli, J.S.Beck, *Nature* 359 (**1992**), 710.
[9] D.Zhao, Q.Huo, J.Feng, B.F.Chmelka, G.D.Stucky, *J. Am. Chem. Soc.* 120 (**1998**), 6024.
[10] D.Zhao, J.Feng, Q.Huo, N.Melosh, G.H.Fredrickson, B.F.Chmelka, G.D.Stucky, *Science* 279 (**1998**), 548.
[11] F.Zhang, Y.Yan, H.Yang, C.Yu, B.Tu, D.Zhao, *J. Phys. Chem. B* 109 (**2005**), 8723.
[12] K.Holmberg, B.Jönsson, B.Kronberg, B.Lindman. **2003**. *Surfactants and polymers in aqueous solution*. 2nd Ed. WILEY.
[13] G.Wanka, H.Hoffmann, W.ulbricht, *Macromolecules* 27 (**1994**), 4145.
[14] Q.Huo, D.I.Margolese, G.D.Stucky, *Chem. Mater.* 8 (**1996**), 1147.
[15] K.M.Ryan, N.R.B.Coleman, D.M.Lyons, J.P.Hanrahan, T.R.Spalding, M.A.Morris, D.C.Steytler, R.K.Heenan, J.Holmes, *Langmuir* 18 (**2002**), 4996.
[16] Q.Cai, Z-S.Luo, W-Q.Pang, Y-W.Fan, X-H.Chen, F-Z.Cui, *Chem. Mater.* 13 (**2001**), 258.
[17] X.Cui, W-C.Zin, W-J.Cho, C-S.Ha, *Materials Letters* 59 (**2005**), 2257.
[18] T.Yamada, H.Zhou, K.Asai, I.Honma, *Materials Letters* 56 (**2002**), 93.
[19] R.D.Schmid, R.Verger, *Angew. Chem. Int. Ed* 37 (**1998**), 1608.
[20] X.Y.Wu, S.Jääskeläinen,Y-Y.Linko, *Appl. Biochem. Biotechnol.* 59 (**1996**), 145.
[21] H.H.P.Yiu, P.A.Wright, *J. Mater. Chem.* 15 (**2005**), 3690.
[22] C-H.Lee, T-S.Lin, C-Y.Mou, *Nano Today* 4 (**2009**), 165.
[23] www.*wikipedia.org*
[24] N.Ravishankar, *J. Phys. Chem. Lett.* 1 (**2010**), 1212.
[25] S.W.Provencher, *Computer Physics Communications* 27 (**1982**), 229.
[26] B.Smarsly, M.Groenewolt, M.Antonietti, *Prog. Colloid Polym. Sci.* 130 (**2005**), 105.
[27] P.C.A.Alberius, K.L.Frindell, R.C.Hayward, E.J.Kramer, G.D.Stucky, B.F.Chmelka, *Chem. Mater.* 14 (**2002**), 3284.
[28] S.Brunauer, P.H.Emmett, E.Teller, *J. Am. Chem. Soc.* 60 (**1938**), 309.
[29] *IUPAC, compendium of chemical terminology* 1976, 46, 77; (**1997**) 2nd Edition.
[30] J.Rouquerol, D.Avnir, C.W.Fairbridge, D.H.Everett, J.H.Haynes, N.Pernicone, J.D.F.Ramsay, K.S.W.Sing, K.K.Unger, *Pure & Appl. Chem.* 66 (**1994**), 1739.
[31] K.S.W.Sing, D.H.Everett, R.A.W.Haul, L.Moscou, R.A.Pierotti, J.Rouquérol, T.Siemieniewska, *Pure & Appl. Chem.* 57 (**1985**), 603.
[32] M-C.Pan,Y-X,Yang, H-P.Ying, X-C.Jia, Y-R.Chen, Y.Tang, *Chinese Journal of Chemistry* 25 (**2007**), 1514.
[33] H-P.Lin, C-P.Kao, C-Y.Mou, *Microporous and Mesoporous Materials* 48 (**2001**), 135.
[34] J.Yun, J-L.Shi, H-R.Chen, J-N.Yan, D-S.Yan, *Microporous and Mesoporous Materials* 46 (**2001**), 153.

[35] M.Hartmann. *Chem. Mater.* 17 (**2005**), 4577.

[36] A.Berggren, A.E.C.Palmqvist, K.Holmberg. *Soft. Mater.* 1 (**2005**), 219.

[37] L.Sierra, B.Lopez, J-L.Guth, *Microporous and Mesoporous Materials* 39 (**2000**), 519.

[38] K.Kosuge, T.Sato, N.Kikukawa, M.Takemori, *Chem. Mater.* 16 (**2004**), 899.

[39] Andreas Sundblom, *formation of mesostructured silica based on non-ionic* interactions, Göteborg (**2010**), p.4 – 6. PhD thesis. Chalmers University of Technology, Department of Chemical and Biological Engineering.

[40] A.Berggren, A.E.C.Palmqvist, *J. Phys. Chem. C* 112 (**2008**), 732.

[41] A.B.D.Nandiyanto, S-G.kim, F.Iskandar, K.Okuyama, *Microporous and Mesoporous Materials* 120 (**2009**), 447.

[42] T.Yokoi, Y.Sakamoto, O.Terasaki, Y.Kubota, T.Okubo, T.Tatsumi, *J. Am. Chem. Soc.* 128 (**2006**), 13664.

[43] C-Y.Mou, H-P.Lin, *Pure Appl. Chem.* 72 (**2000**), 137.

[44] R.I.Nooney, D.Thirunavukkkarasu, Y.Chen, R.Josephs, A.E.Ostafin, *Chem. Mater.* 14 (**2002**), 4721.

[45] K.Suzuki, K.Ikari, H.Imai, *J. Am. Chem. Soc.* 126 (**2004**), 462.

[46] J.Sun, H.Zhang, R.Tian, D.Ma, X.Bao, D-S.Su, H.Zou, *Chem. Commun.* (**2006**), 1322.

[47] J.Sun, H.Zhang, D.Ma, Y.Chen, X.Bao, A.Klein.Hoffmann, N.Pfänder, D.S.Su. *Royal Soc. Of Chem.* (**2005**), 5343.

[48] E.M.Johansson, J.M.Córdoba, M.Odén, *Microporous and Mesoporous Materials* 133 (**2010**), 66.

[49] H.Zhang, J.Sun, D.Ma, X.Bao, A.Klein-Hoffmann, G.Weinberg, D.Su, R.Schlögl, *J. Am. Chem. Soc.* 126 (**2004**), 7440.

[50]